In vitro and in vivo studies of artemisinin endoperoxides

Therese Ericsson

Department of Pharmacology
Institute of Neuroscience and Physiology
Sahlgrenska Academy at University of Gothenburg

UNIVERSITY OF GOTHENBURG

Gothenburg 2014

Cover illustration: Molecular structure of artemisinin, the original compound of the artemisinin class of endoperoxides.

In vitro and in vivo studies of artemisinin endoperoxides

ericsson.therese@gmail.com

ISBN 978-91-628-9078-0
ISBN 978-91-628-9082-7 (pdf)
http://hdl.handle.net/2077/35949

Printed in Gothenburg, Sweden 2014
Kompendiet, Aidla Trading AB, Gothenburg, Sweden

To my beloved family

As far as the laws of mathematics refer to reality, they are not certain, as far as they are certain, they do not refer to reality.

Albert Einstein

In vitro and in vivo studies of artemisinin endoperoxides

Therese Ericsson

Department of Pharmacology, Institute of Neuroscience and Physiology
Sahlgrenska Academy at University of Gothenburg
Gothenburg, Sweden

ABSTRACT

Artemisinin and its semi-synthetic derivatives (eg. Artemether/ARM, artesunate/ARS, dihydroartemisinin/DHA) play an important role in combating malaria, and treatments containing an artemisinin derivative (artemisinin-based combination therapies, ACTs) are today the standard treatment worldwide for *Plasmodium falciparum* malaria. In addition to their antimalarial effect, these compounds have been demonstrated to exert cytotoxic effects, making them interesting candidates for oncologic indications.

This thesis specifically aimed to (1) investigate *in vitro* effects of artemisinin endoperoxides on human liver Cytochrome P450 (CYP) enzyme activity, and to (2) study the pharmacokinetics of ARS and DHA in plasma and saliva during long-term oral ARS treatment in patients with breast cancer. *In vitro* experimental assays using recombinant and microsomal CYP enzymes were conducted to assess potential inhibitory effects of artemisinin, ARM, ARS and DHA (**Papers I** and **II**). Results were extrapolated to evaluate the risk of drug-drug interactions (DDIs) *in vivo*. An LC-MS/MS method was optimized and validated for the quantification of ARS and DHA in human plasma and saliva (**Paper III**). Drug concentration-time profile data was analyzed by non-compartmental analysis (**Paper IV**) and population pharmacokinetic modelling (**Paper V**) to characterize the pharmacokinetic properties of the two compounds in patients with breast cancer, and to evaluate the relationship between salivary and plasma DHA concentrations.

In conclusion, artemisinin endoperoxides exert inhibitory effects on the activity of CYP enzymes *in vitro*, which could result in clinically significant DDIs. This could be a concern in both malaria and cancer therapies, which often include concomitant administration of multiple drugs. Also, for the first time, the presented bioanalytical method offers the possibility to quantify ARS and DHA in saliva. Therefore, based on both plasma and saliva data, the

pharmacokinetics of the two compounds have been characterized during long-term oral ARS treatment in patients with breast cancer. Prior knowledge regarding the pharmacokinetics of these antimalarial drugs is based on single dose or short-term (≤7 days) regimens in healthy volunteers or in malaria patients, making the results presented here significant.

Keywords: artemisinin, artesunate, breast cancer, Cytochrome P450, dihydroartemisinin, inhibition, LC-MS/MS, pharmacokinetics, plasma, saliva

ISBN: 978-91-628-9078-0

SAMMANFATTNING PÅ SVENSKA

Denna avhandling belyser *in vitro* och *in vivo* aspekter kring artemisinin-baserade läkemedel. Artemisinin är en naturligt förekommande substans som kan utvinnas ifrån den kinesiska medicinalväxten sommarmalört (*Artemisia Annua* L.), en ört som i över tvåtusen år har använts i syfte att lindra frossa och feber. Semisyntetiska derivat av artemisinin, såsom artemeter (ARM), artesunat (ARS) och dihydroartemisinin (DHA), har under den senaste tiden utvecklats och tillhör, liksom modersubstansen, den kemiska gruppen endoperoxider. Utöver antimalariaeffekt så har dessa föreningar även visat sig ha hämmande effekter på många tumörceller. Detta, tillsammans med föreningarnas relativt milda biverkningsprofil, gör dem till intressanta kandidater även inom cancerbehandling.

I den inledande delen av denna avhandling (**artiklar I** och **II**) utvärderades artemisininbaserade läkemedel för deras potentiella inhibitoriska effekter på läkemedelsnedbrytande enzymer som kallas för Cytokrom P450 (CYP). Baserat på experimentella provrörsförsök (*in vitro*), visade sig att samtliga utvärderade endoperoxider har en hämmande effekt på aktiviteten av flertalet CYP-enzymer. Detta skulle kunna resultera i ogynnsamma effekter (otillräcklig terapeutisk effekt eller toxiska effekter) vid samtidig administrering av dessa föreningar med andra läkemedel i patienter (*in vivo*).

I den andra delen av denna avhandling har en bioanalytisk metod med hög känslighet baserad på LC-MS utvecklats och validerats för kvantifiering av ARS och DHA i human plasma och saliv (**artikel III**). Metoden tillämpades på kliniska prover ifrån en klinisk studie genomförd vid Heidelbergs universitet. Studien omfattade 23 bröstcancerpatienter som fick genomgå långtidsbehandling (>3 veckor) med oralt ARS givet i tablettform en gång dagligen. Koncentrationen i plasma och saliv togs fram och analyserades dels med enklare datamodellering (**artikel IV**) samt med mer modellbaserad analys (**artikel V**) för att karaktärisera de farmakokinetiska egenskaperna för ARS (administrerat läkemedel) och den bildade aktiva metaboliten DHA i den givna patientpopulationen. Sambandet mellan läkemedelskoncentrationer i saliv och plasma studerades för att utvärdera möjligheten till salivprovtagning för analys av dessa substanser (**artikel V**).

Sammanfattningsvis har denna avhandling visat att studerade artemisininbaserade läkemedel utövar hämmande effekter på viktiga CYP-enzymer. Den beskrivna bioanalysmetoden möjliggör, för första gången, kvantifiering av ARS och DHA i human saliv. Detta har medfört en

genomgående karaktärisering av farmakokinetiska egenskaper hos dessa två föreningar i bröstcancerpatienter under långtidsbehandling, vilket tidigare ej har studerats. Intressanta resultat visar på en tidsberoende kinetik för den aktiva metaboliten DHA, där en ökande elimination av substansen föreligger vid upprepad oral administrering av ARS under längre tid (> 3 veckor). Detta har sedan tidigare visats för flera artemisininbaserade läkemedel, en effekt som har tillskrivits (auto)induktion av de CYP-enzym som bidrar till föreningarnas elimination. Autoinduktion, skulle kunna vara den bakomliggande mekanismen för en ökande elimination av DHA som beskrivits i detta arbete.

LIST OF PAPERS

This thesis is based on the following studies, referred to in the text by their Roman numerals.

I. **Ericsson T**, Masimirembwa C, Abelo A, Ashton M. The evaluation of CYP2B6 inhibition by artemisinin antimalarials in recombinant enzymes and human liver microsomes. *Drug Metab Lett.* 2012;6(4):247-57

II. **Ericsson T**, Sundell J, Torkelsson A, Hoffmann KJ, Ashton M. Effects of artemisinin antimalarials on Cytochrome P450 enzymes *in vitro* using recombinant enzymes and human liver microsomes: potential implications for combination therapies. *Xenobiotica*. 2014:Jul;44(7):615-26

III. Birgersson S, **Ericsson T**, Blank A, von Hagens C, Ashton M, Hoffmann KJ. A high-throughput liquid chromatographic-tandem mass spectrometric method for quantification of artesunate and its metabolite dihydroartemisinin in human plasma and saliva. *Bioanalysis*. 2014:doi:10.4155/BIO.14.116 (*In press*)

IV. Blank A, **Ericsson T**, Walter Sack I, Markert C, Burhenne J, von Hagens C, Ashton M, Edler L, Haefeli WE, Mikus G. Pharmacokinetics of artesunate and its active metabolite dihydroartemisinin in prolonged use in patients with metastatic breast cancer. (*Submitted*)

V. **Ericsson T**, Blank A, von Hagens C, Ashton M, Abelo A. Population pharmacokinetics of artesunate and dihydroartemisinin during long-term oral administration of artesunate to patients with metastatic breast cancer. (*Submitted*)

CONTENT

ABBREVIATIONS XIII
DEFINITIONS IN SHORT XVII
1 INTRODUCTION 1
1.1 Artemisinin and derivatives 1
1.1.1 Chemistry, general properties and mechanism of action 1
1.1.2 Artemisinin-based combination therapies (ACTs) 3
1.1.3 Clinical safety and toxicity of artemisinins 4
1.1.4 Pharmacokinetics of artesunate and dihydroartemisinin 5
1.1.5 Artemisinins in cancer 6
1.2 Drug Metabolism 9
1.2.1 Human Cytochrome P450 enzymes 9
1.2.2 Modification of CYP activity and the risk of drug-drug interactions 11
1.2.3 *In vitro* methods for CYP inhibition 14
1.2.4 *In vitro-in vivo* extrapolation 15
1.3 Drug concentration monitoring 16
1.4 Bioanalytical method validation 17
1.5 Pharmacometrics 18
1.5.1 Population pharmacokinetics 19
1.5.2 Nonlinear mixed-effects modelling 19
2 AIM 22
3 METHODS 23
3.1 Paper I and II - CYP inhibition studies 23
3.1.1 Recombinant enzyme incubations 23
3.1.2 Microsomal incubations 23
3.1.3 Analytical methods 24
3.1.4 Data analysis 27

3.2 Paper III - Bioanalytical method for quantification of ARS and DHA in human plasma and saliva 29
3.2.1 Instrumentation 29
3.2.2 Sample preparation and LC-MS/MS assay 29
3.2.3 Method validation 30
3.2.4 Application to clinical plasma and saliva samples 30
3.3 Paper IV – Pharmacokinetics of ARS and DHA in patients with breast cancer 30
3.3.1 Study design 30
3.3.2 Pharmacokinetic analysis 31
3.4 Paper V - Population pharmacokinetics of ARS and DHA in patients with breast cancer 31
3.4.1 Study design 31
3.4.2 Model development 32
3.4.3 Data analysis 34
4 RESULTS 35
4.1 Paper I – CYP2B6 inhibition by artemisinin antimalarials *in vitro* 35
4.1.1 Recombinant CYP2B6 (rCYP2B6) activity 35
4.1.2 Microsomal CYP2B6 activity 37
4.1.3 Predicted change in drug exposure *in vivo* 37
4.2 Paper II – CYP inhibition by artemisinin antimalarials *in vitro* 38
4.2.1 Recombinant CYP (rCYP) activity 38
4.2.2 Microsomal CYP activity 38
4.2.3 Predicted change in drug exposure *in vivo* 40
4.3 Paper III - Bioanalytical method for quantification of ARS and DHA in human plasma and saliva 43
4.3.1 Sample preparation and LC-MS/MS assay 43
4.3.2 Method validation 43
4.3.3 Application to clinical plasma and saliva samples 44
4.4 Paper IV – Pharmacokinetics of ARS and DHA in patients with breast cancer 47

4.5 Paper V - Population pharmacokinetics of ARS and DHA in patients with breast cancer 51
5 DISCUSSION 56
6 CONCLUSION 59
7 FUTURE PERSPECTIVES 61
ACKNOWLEDGEMENT 62
REFERENCES 65
SUPPLEMENTARY MATERIALS 73

ABBREVIATIONS

ACTs	Artemisinin-based combination therapies
AhR	Aryl hydrocarbon receptor
AIC	Akaike information criterion
ARM	Artemether
ARTIC (study)	Artesunate in breast cancer
ARS	Artesunate
ALAT	Alanine aminotransferase
ASAT	Aspartate aminotransferase
AUC	Area under the drug concentration-time curve
BQL	Below limit of quantification
BSV	Between-subject variability
BW	Body weight
CAR	Constitutive androstane receptor
CI	Confidence interval
CL	Clearance
CL/F	Apparent/oral clearance (elimination clearance)
C_{max}	Maximal drug concentration
%CV	Coefficient of variation
CYP	Cytochrome P450
DDI	Drug-drug interaction

DHA	Dihydroartemisinin
DHA(P)	Total plasma concentration of DHA
DHA(S)	DHA concentration in saliva
E_0	Maximal enzyme activity in the absence of inhibitor
E_{max}	Maximum drug induced inhibition of the enzyme activity
ESI	Electrospray ionization
F	Relative bioavailability
FDA	Food and Drug Administration
f_H	Fraction of drug eliminated by metabolism
f_m	Fraction of metabolic clearance which is subject to inhibition
FOCE	First-order conditional estimation
G-6-P	Glucose-6-phosphate
G-6-P-D	Glucose-6-phosphate dehydrogenase
GOF	Goodness-of-fit
HLM	Human liver microsomes
HPLC	High-performance liquid chromatography
[I]	*In vivo* concentration of an inhibitory compound
$[I]_{max,u}$	Maximum unbound systemic inhibitor concentration
$[I]_{max,inlet,u}$	Maximum unbound inhibitor concentration at the inlet to the liver
IC_{50}	Half maximal inhibitory concentration
IS	Internal standard

IVIVE	*In vitro-in vivo* extrapolation
k_a	First-order absorption rate constant
K_i	Inhibition constant
K_m	Michaelis-Menten constant
LC-MS/MS	Liquid chromatography/tandem mass spectrometry
LLOQ	Lower limit of quantification
MRM	Multiple reaction monitoring
m/z	Mass-to-charge ratio
NCA	Non-compartmental analysis
$NADP^+$	Nicotinamide adenine dinucleotide phosphate
NADPH	Reduced form of $NADP^+$
OFV	Objective function value
P450s	Cytochrome P450 enzymes
PfATP6	*P. falciparum* calcium-dependent ATPase
PPAR	Peroxisome proliferator-activated receptor
PXR	Pregnane X receptor
QC	Quality control
Q/F	Intercompartmental clearance
rCYP	Recombinant CYP enzymes
%RE	Relative error
ROS	Radical oxygen species
%RSE	Relative standard error

RXR	Retinoid X receptor
SD	Single dose (Paper IV)
SD	Standard deviation
SE	Standard error
SS	Steady state
SPE	Solid phase extraction
TDI	Time-dependent inhibition
$t_{1/2}$	Elimination half-life
T_{max}	Time to reach maximal drug concentration
UGT	UDP-glucuronosyltransferase
V	Rate of metabolite formation
V/F	Apparent volume of distribution
V_C/F	Apparent volume of distribution of the central compartment
V_P/F	Apparent volume of distribution of a peripheral compartment
V_{max}	Maximal rate of metabolite formation
VPC	Visual predictive check
WHO	The World Health Organization
ε	Residual random error
η	Deviation of an individual parameter estimate from the estimated population mean of the parameter; a term that describes the between-subject variability
θ_{pop}	Estimated population mean of a pharmacokinetic parameter

DEFINITIONS IN SHORT

Pharmacodynamics	How the drug affect the body [1]. The study of a drug's pharmacological effect on the body.
Pharmacokinetics	How the body handles the drug [1]. The study of how the body affects a specific drug after administration through the mechanisms of absorption, distribution, metabolism, and excretion.
Pharmacometrics	Branch of science concerned with mathematical models of biology, pharmacology, disease, and physiology used to describe and quantify interactions between xenobiotics and patients, including beneficial effects and side effects resultant from such interfaces [2]
Population pharmacokinetics	The study of pharmacokinetics at the population level. Seeks to quantify and explain variability in drug exposure among individuals in a population [3-4].

1 INTRODUCTION

The use of the artemisinin class of endoperoxides is widely accepted as the first line treatment of malaria. The World Health Organization (WHO) recommends artemisinin-based combination therapy (ACT) for the treatment of uncomplicated *Plasmodium falciparum* malaria to improve the treatment outcome and counteract the threat of resistance development [5]. In addition to antimalarial activity, the artemisinin class of endoperoxides has been shown to exert cytotoxic effects, and lately, considerable attention has been focused on the demonstrated anticancer properties of these compounds [6-7].

1.1 Artemisinin and derivatives

1.1.1 Chemistry, general properties and mechanism of action

Artemisinin is a naturally occurring sesquiterpene lactone endoperoxide derived from the Chinese medicinal herb qinghao (*Artemisia annua* L.). This plant has been used in traditional Chinese medicine for more than 2000 years in the treatment of fever, but it was not until 1972 that the active antimalarial moiety, artemisinin, was isolated from the leaves and the structure was identified [8-9]. The highly lipophilic compound exhibits low solubility in both oil and water, restricting artemisinin to be developed as an oral formulation, thereby limiting its therapeutic use. Several semi-synthetic derivatives, such as artemether (ARM), artesunate (ARS) and dihydroartemisinin (DHA) (Fig. 1) have been developed to enable not only oral, but also rectal, intramuscular, or intravenous administration [9]. The reduction of a ketogroup in artemisinin with sodium borohydride to the corresponding alcohol results in the formation of the more potent derivative DHA [10]. With DHA as an intermediate, ARM and ARS are synthesized through the etherification with methanol and the esterification with succinic acid anhydride, respectively [10]. The oil-soluble ARM has been synthesized for oral, rectal and intramuscular use, while the water-soluble ARS can be administrated orally, rectally, intramuscularly or intravenously. Both ARM and ARS are metabolized *in vivo* to DHA, which appears to be the principle bioactive metabolite in plasma [8, 11]. Consequently, ARS can be considered a prodrug for DHA, being rapidly and almost completely hydrolyzed to the metabolite, which is the main contributor to the overall antimalarial activity [8, 12-13]. Depending on the route of administration the conversion of ARS to DHA can be both through pH-dependent chemical hydrolysis and/or

enzymatic deesterification catalyzed by blood esterases [8, 11]. The biotransformation of ARM to DHA is slower and less complete than that of ARS, and the demethylation of ARM is catalyzed by the Cytochrome P450 enzyme system (CYP1A2, 2B6, 3A4) [8, 11, 13].

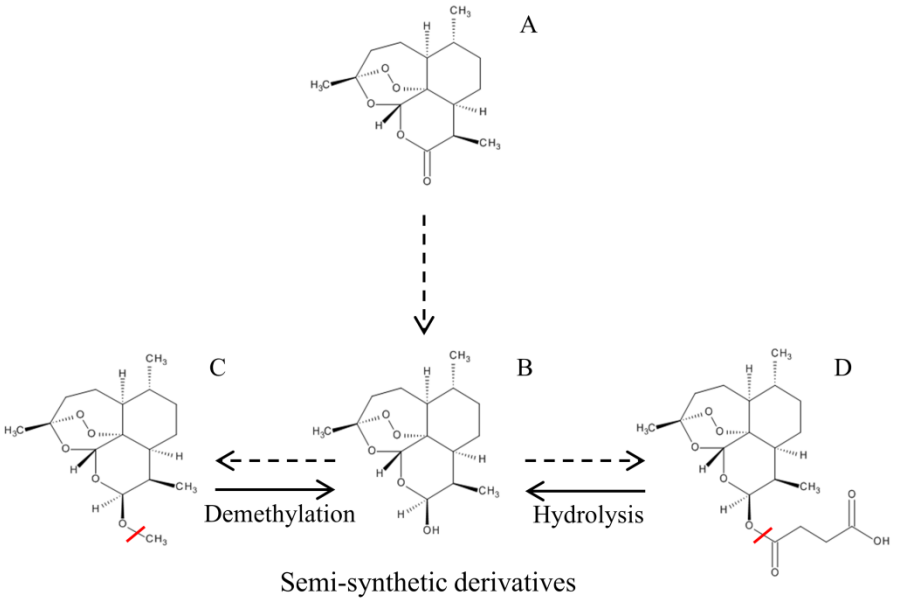

Figure 1. Chemical structures of (A) artemisinin and its semi-synthetic derivatives (dashed arrows) (B) dihydroartemisinin (DHA), (C) artemether (ARM) and (D) artesunate (ARS), also known as artesunic acid. DHA is the active metabolite of both ARM and ARS, formed through CYP-mediated demethylation of ARM and through chemical or enzymatic hydrolysis of the ester function in ARS.

Common to all artemisinin class of compounds is the endoperoxide bridge, which is essential for antimalarial activity. However, the exact mechanism of action for these compounds is still unresolved, and several hypotheses have been proposed. One theory is the iron-mediated cleavage of the endoperoxide bridge and the subsequent formation of reactive oxygen-centered radicals which rapidly rearrange to more stable carbon-centered radicals. These radicals as reactive intermediates have been suggested to alkylate and inhibit a variety of parasite molecules, resulting in parasite´s death. It has been hypothesized that heme, a cellular component that accumulates in the malaria parasite as a result of hemoglobin digestion, is a rich source of intracellular iron (Fe^{2+}) that activates artemisinins inside the parasite. An alternative

theory is that artemisinins exert their antimalarial activity by selectively and irreversibly binding to and inhibiting the PfATP6 (a *P. falciparum* calcium-dependent ATPase) in the endoplasmatic reticulum. This inhibition has been shown to be Fe^{2+}-dependent and the loss of PfATP6 function results in parasite death. These theories and other hypothesis on the mechanism of action for the artemisinin endoperoxides have been reviewed elsewhere [9, 14-15].

The artemisinin class of compounds is potent against all *Plasmodium* parasites, including otherwise multidrug-resistant *P. falciparum* [9]. The compounds inhibit the early stage of parasite development once parasites have invaded red blood cells, but also slow down early sexual-stage (gametocyte) development and therefore have a potential to reduce transmission. However, they do not kill the hepatic stage of the parasite [9, 14].

1.1.2 Artemisinin-based combination therapies (ACTs)

Malaria is an entirely preventable and treatable disease if prompt and effective treatment is initiated at an early stage of the infection. However, if treatment is delayed or if ineffective medicines are given, severe malaria may be manifested, which dramatically increases the mortality [5, 16]. The misuse and the extensive deployment of antimalarial drugs have provided an enormous selection pressure on human malarial parasites, particularly *P. falciparum*, contributing to the emergence of resistance. To combat the spread of resistance, the use of combination drug therapies is highly employed in malarial treatment. The concept behind combination treatments is that a single point mutation in the parasite genome may not provide protective cover to the parasite when two drugs are administrated. The risk of developing resistance to two drugs with different modes of action, and therefore different resistance mechanisms, is significantly less than to one drug [17].

The artemisinin-related endoperoxides are the most important class of anti-malarial drugs with a rapid onset of antimalarial effect, resulting in a fast decline in the number of parasites. When given as monotherapy, the artemisinins are associated with a high risk of recrudescence due to their short half-lives and failure to eliminate all parasites [9, 14]. Therefore, artemisinins are recommended to be used in combination with another effective, longer-acting antimalarial drug to completely eliminate the parasites and prevent the emergence of resistant *P. falciparum*. The ACTs

that are recommended in the treatment of uncomplicated *P. falciparum* malaria include ARM-lumefantrine, ARS-amodiaquine, ARS-mefloquine, ARS-sulfadoxine/pyrimethamine and DHA-piperaquine [5].

1.1.3 Clinical safety and toxicity of artemisinins

When used in short-term treatment of malaria, the artemisinin endoperoxides are safe and well-tolerated drugs. Many clinical trials involving artemisinin and its structural analogues have been conducted, indicating high tolerability and safety of these compounds in different populations [18-22]. Despite pre-clinical signs of neurotoxicity observed in animal models, the artemisinin class of compounds has been found to be virtually void of any serious side effects in humans [23]. Olliaro *et al.* reported no serious adverse events or severe toxicity in a systematic review of 108 published and unpublished clinical trials involving artemisinin endoperoxides conducted in healthy subjects and patients with uncomplicated or severe malaria [24]. The most common adverse events reported were gastrointestinal-related. Similarly, Price *et al.* reported the safety and tolerability of oral ARS and ARM in a systemic review on the adverse effects of the two artemisinin derivatives, either as monotherapy or in combination with mefloquine [25]. The combination regimens were associated with more side effects, such as acute nausea, vomiting, anorexia and dizziness, than the monotherapies. However, no evidence of neurotoxicity was reported for any of the derivatives.

The neurotoxicity seen in experimental animals, but not in humans, can most likely be explained by higher pre-clinical doses compared to those used in clinic, in addition to differences in the pharmacokinetic profiles after different routes of administrations [23]. The toxicity is related to the presence of artemisinin endoperoxides for a long period of time, and in particular, the neurotoxicity in animals has been associated with intramuscular ARM or arteether [25-26]. These are oil-based compounds that are released relatively slowly from the intramuscular injection site, resulting in persistent drug concentrations after repeated intramuscular administrations. On the other hand, intramuscular ARS has been shown to be less neurotoxic than intramuscular ARM in experimental animal models, probably due to its water solubility and rapid absorption [27]. In humans, the most commonly used route of administration is oral intake, resulting in fast absorption and elimination of the artemisinin endoperoxides, which probably explains the lack of neurotoxicity findings in humans [23].

1.1.4 Pharmacokinetics of artesunate and dihydroartemisinin

As a consequence of the chemical and enzymatic hydrolysis of ARS to DHA, the plasma drug concentration profiles of both parent compound and metabolite are affected by the combined effects of (i) biotransformation occurring in both the gastrointestinal tract and the systemic circulation (chemical and/or enzymatic hydrolysis); and (ii) different rates of absorption of ARS and DHA [8].

The clinical pharmacokinetics of ARS and DHA have been reviewed by Fleckenstein and colleagues [28]. Following oral administration, the absorption of ARS is rapid, supported by the findings that ARS is detectable in plasma soon after dosing, often within 15 minutes post-dose, and with peak plasma concentrations (T_{max}) within the first hour after dose [28]. ARS as a prodrug, is considered to be completely biotransformed to its active metabolite, and the oral bioavailability of DHA relative to intravenous administration was reported to be 82% in adults with uncomplicated *P. falciparum* malaria [29], and 85% in adults with *P. vivax* malaria [30]. Following oral ARS administration, the exposure (C_{max} and AUC) of DHA is higher than that of the parent compound, with peak plasma concentrations typically occuring within two hours post-dose [28]. Elimination of the metabolite is somewhat slower than that of the parent compound following oral ARS administration, with half-lives of 0.5-1.5 hours and 20-45 minutes for DHA and ARS, respectively [28].

There are fewer published estimates of the apparent clearance and volume of distribution of ARS than for its metabolite. Due to its rapid conversion to DHA and the subsequent decline in plasma levels, ARS requires sensitive bioassays to be detected in clinical samples. Consequently, many pharmacokinetic studies of ARS only report the pharmacokinetic parameters of DHA.

Teja-Isavadharm and colleagues reported a mean apparent clearance (CL/F) and volume of distribution (V/F) for ARS to be 20.6 L/hr/kg and 14.8 L/kg, respectively, in six healthy Thai volunteers following oral ARS [31]. In the same study, mean CL/F and V/F for DHA were determined to be 2.42 L/hr/kg and 3.02 L/kg, in healthy subjects, and 1.22 L/hr/kg and 1.33 L/kg in patients with *P. falciparum* malaria, respectively.

Following oral ARS administration in healthy volunteers, Orrell *et al.* reported an average oral volume of distribution and clearance for DHA to be

0.073 L/kg and 2.2 L/hr/kg, respectively (values adjusted for mean body weight of the study participants; 67.3 kg) [32]. No corresponding estimates for ARS V/F and CL/F were reported.

Davis *et al.* reported the pharmacokinetics of ARS and DHA following a three day regimen of oral ARS in healthy male volunteers [33]. Due to low ARS concentrations in the clinical samples, the apparent clearance and volume of distribution were not determined for the parent compound but only for the metabolite. No significant difference in the pharmacokinetics of DHA between day 1 and day 3 was observed, with CL/F and V/F determined to 1.07 vs. 1.45 L/h/kg and 2.26 vs. 2.39 L/kg, respectively (values adjusted for mean body weight of the study participants; 77 kg).

Based on population pharmacokinetic analysis Tan and colleagues reported the apparent clearance (CL/F) and the volume of distribution (V/F) for ARS to be 19.3 L/hr/kg and 19.8 L/kg, respectively, following oral ARS in healthy volunteers (values adjusted for median weight in the population; 61.5 kg) [34]. For DHA, the population estimates of central apparent clearance and central volume of distribution were 1.52 L/hr/kg and 1.58 L/kg, respectively, with body weight as a significant covariate on DHA apparent clearance.

1.1.5 Artemisinins in cancer

Besides the use in malaria treatment, convincing evidence has emerged showing that artemisinin-related compounds exert cytotoxic effects against cancer cells. Cytotoxicity has been demonstrated *in vitro* in a variety of human cancer cell types and *in vivo* in different animal models [35-40]. Some clinical reports also demonstrate anticancer effects by artemisinin endoperoxides in human beings [41-44]. The inhibitory effect on cancer cells exerted by artemisinins often requires higher concentrations (nano- to micromolar range) than the cytotoxic effect against *Plasmodium* parasites [45]. However, because of the favorable safety profiles of artemisinin endoperoxides, they would likely be well tolerated in cancer treatment and pose minimal risk to patients, provided that higher doses in combination with long-term exposure will not increase the safety risk. If they prove to have anti-cancer activity, artemisinin endoperoxides would be good candidates for adjunctive therapy against various cancers.

Cytotoxic agents frequently exert their effects on tumor cells through several mechanisms and cellular responses to the drugs are multi-factorial. As with the antimalarial activity exerted by artemisinin endoperoxides, the mechanism underlying their cytotoxic effects against cancer cells is

debatable. The antiparasitic activity and the anticancer effects share a common pharmacophore, with the endoperoxide function at least partly responsible for the growth inhibitory effect on cancer cells. Lack of this particular chemical bond significantly reduces the cytotoxic effects against cancer cells [45-46]. It has been hypothesized that the cytotoxicity and selectivity is dependent upon higher iron load in cancer cells, which is a requirement to maintain continued growth and proliferation [47]. The high concentrations of iron in cancer cells facilitate the cleavage of the endoperoxide bridge with subsequent release of carbon-centered radicals and radical oxygen species (ROS), resulting in oxidative damage [7, 45]. Mercer *et al.* investigated the bioactivation of the endoperoxide moiety and subsequent cell death *in vitro* in order to determine mammalian cell susceptibility to artemisinins [48]. The bioactivation of the endoperoxide group was shown to be dependent upon cellular heme, and an early subsequent generation of ROS was suggested to be an important initiating event in the induction of apoptotic cell death. Inhibition of both heme synthesis and ROS generation separately resulted in decreased cytotoxicity. These findings further support the hypothesis that the chemical basis of ARS-induced cytotoxicity is a cellular heme dependent bioactivation of the endoperoxide group and a subsequent generation of ROS.

The cellular response to artemisinin endoperoxides in cancer cells includes growth inhibition by regulation of nuclear receptor responsiveness, induction of apoptosis, cell cycle arrest, disruption of cell migration, and inhibition of angiogenesis. These effects results from the interference of artemisinins with a range of signaling pathways involved in malignancy. The antitumor effects and proposed mechanisms of action of artemisinins in cancer cells have been reviewed elsewhere [6-7, 45].

Documented antitumor activity *in vitro* and in animal models indicates that ARS and DHA are the most active artemisinin endoperoxides, and quite extensive research has been focused on their anticancer effects [45]. ARS-induced cytotoxicity has been found in a variety of cell lines from different tumor types, including e.g. brain, breast, colon, leukemia, lung, melanoma, prostate and pancreas [35, 49]. An increased inhibition rate in the majority of the tested cell lines was observed when ARS was combined with iron(II) glycine sulfate compared to ARS alone, indicating an enhanced susceptibility of tumor cells to ARS by ferrous iron [49].

In the systemic circulation, iron is transported bound to the protein transferrin, which upon binding to the transferrin receptor 1 delivers iron to the cells by receptor-mediated endocytosis [47]. Iron is essential for the

activity of multiple metabolic processes involved in cell growth and proliferation. To maintain their rapid rate of division, cancer cells generally express higher cell surface concentrations of transferrin receptors than normal cells, resulting in higher rates of iron load [47]. This may contribute to the selectivity of artemisinins-induced toxicity to cancer cells. *In vitro* studies indicate that DHA combined with holotransferrin (i.e. iron loaded transferrin) is selectively toxic to human breast cancer cells, with low toxicity against normal breast cells [50]. Presence of holotransferrin further increased the cytotoxicity of DHA to breast cancer cells compared to when exposed to DHA alone. Lai *et al.* also reported a growth retardation of breast tumors in the rat after daily intravenous injection of artemisinin-transferrin conjugate compared to control [40]. The artemisinin-transferrin complex utilizes the transferrin receptor mechanism to deliver artemisinin into cancer cells. In the same study, oral DHA was also reported to cause retardation of tumor growth, but to a lesser extent than that observed with the artemisinin-transferrin conjugate. In another *in vivo* study rats implanted with fibrosarcoma were treated with DHA [51]. Oral administration of iron (ferrus sulfate) enhanced the effect of DHA in retarding tumor growth, indicating the role of iron in the cytotoxicity of artemisinin endoperoxides toward cancer cells.

1.2 Drug Metabolism

During drug development, hydrophobicity is an important chemical characteristic to consider, with a tendency of an increase in both oral absorption and interaction with molecular target as hydrophobicity increases [52]. However, this also has an impact on the elimination of drugs from the body, with hydrophobic compounds requiring to be biotransformed to more hydrophilic molecules, before they can be renally or biliary excreted. Traditionally, drug metabolism is divided into phase I and phase II reactions [53]. Phase I metabolism includes oxidation, reduction, and hydrolysis reactions, which expose or introduce a functional group on a xenobiotic molecule. This is commonly followed by phase II metabolism, which conjugates the molecule with endogenous substrates (e.g. glucuronic acid, sulfuric acid, amino acid) to form a more hydrophilic metabolite for excretion. However, phase II reactions must not always be preceded by phase I metabolism, but may occur independently.

1.2.1 Human Cytochrome P450 enzymes

The Cytochrome P450 (CYP) enzyme system constitutes a superfamily of isoforms, which are responsible for the oxidative metabolism of >75% of commonly prescribed drugs [53]. The main location of human P450s and the principle site of drug metabolizing activity is the liver. Here, the enzymes are located primarily in the endoplasmatic reticulum. However, some CYP enzymes are also found in the gut wall, contributing to intestinal first-pass metabolism that has been shown to be of clinical relevance for several drugs (Fig. 2). Drug metabolizing CYPs are also distributed to many other tissues throughout the body (e.g. placenta, lung, kidney, brain, adrenal gland, gonads, heart, nasal and tracheal mucosa, and skin), but to a lesser extent [52, 54].

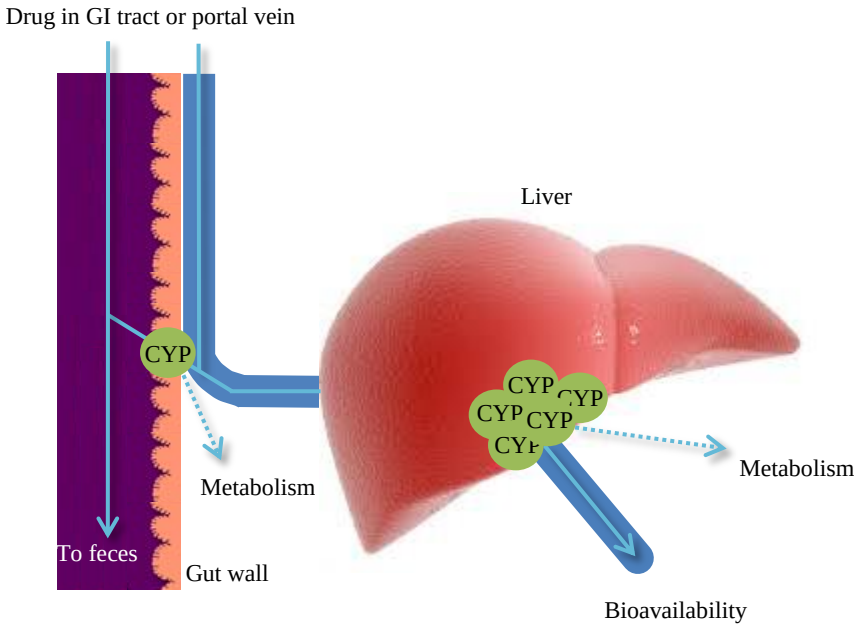

Figure 2. CYP-mediated, pre-systemic biotransformation of drugs may occur in the liver, which is the main location of human P450s. Orally administrated drugs may also be subject to intestinal first-pass metabolism, mediated by CYP enzymes located in the epithelial cells of the upper portions of the intestines.

Three of the human CYP enzyme families (CYP1, CYP2 and CYP3) are responsible for the majority of the hepatic oxidative metabolism of xenobiotics (Fig. 3), with members in the CYP3A family being the most important, followed by the isoforms CYP2D6 and CYP2C9 [52]. CYP2B6 accounts for less than 5% of the total human liver P450 content, and was initially thought to play a rather insignificant role in overall drug metabolism. However, several clinically important drugs, including efavirenz, cyclophosphamide, ifosfamide, bupropion, pethidine, ketamine, propofol, methadone and selegiline, have been identified as CYP2B6 substrates [55-58]. CYP2B6 has also been shown to play an important role in the metabolism of artemisinin and some of its derivatives [8, 59-60].

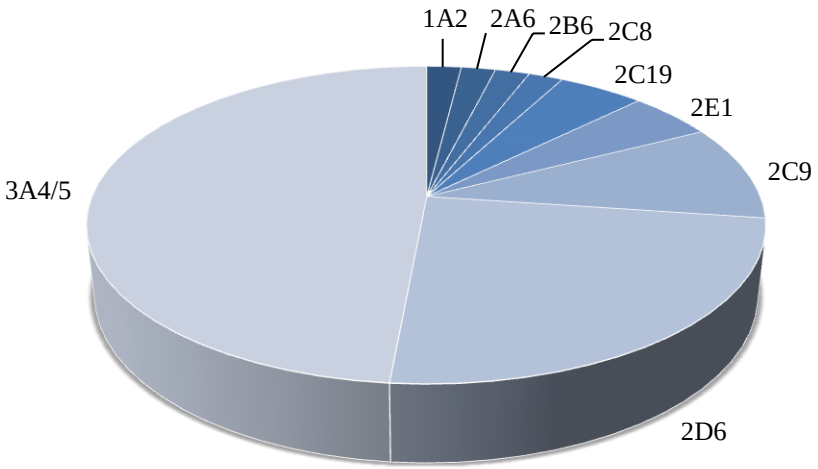

Figure 3. The major CYP enzymes and their approximate contribution to human xenobiotic metabolism. Data derived from Hacker, M., Pharmacology - Principles and Practice (2009).

1.2.2 Modification of CYP activity and the risk of drug–drug interactions

The Cytochrome P450 enzyme system is subject to environmental, biological and genetic influence, resulting in extensive variability in drug metabolizing capacity [54]. Whenever two or more drugs are concomitantly administrated, there is a risk of drug-drug interactions (DDIs), many of which are associated with alterations in metabolic activity of CYP enzymes [61]. Modification of drug metabolizing enzyme activity, either by inhibition or by induction, may have significant implications on the pharmacokinetics and toxicity of drugs. The clinically importance of such interactions depends on, among many other factors, the therapeutic index of drugs [61-62]. Drugs with a small difference between toxic and effective concentrations are more likely to be involved in drug interactions with serious clinical outcome, as their pharmacological activity can change significantly even if only moderate changes in drug metabolism occur.

Inhibition of CYP enzymes

Inhibition of the enzymatic activity of P450s is the most common cause of clinically relevant DDIs [54, 61]. This generally involves a direct interaction between the CYP enzyme and the inhibitory compound, resulting in a rapid onset of the inhibition [63]. Drugs that are extensively metabolized by the inhibited enzyme can accumulate to toxic concentrations and cause serious adverse effects. Because of this, DDIs involving enzyme inhibition are probably of greater clinical importance than those involving enzyme induction [62]. The clinical significance of an enzyme inhibition depends in part on the contribution of the affected enzyme to the overall metabolic elimination of a drug. If the inhibited enzyme is the only route of metabolism of a drug, a clinically significant interaction is expected. However, for most drugs several metabolic routes are involved in the elimination, and inhibition of a single enzyme would be less likely to produce a significant interaction, unless the inhibited pathway contributes to more than 50% of overall elimination. In general, metabolism results in compounds that are less pharmacologically active than the original compound. However, in the case of pro-drugs, which require metabolic biotransformation for therapeutic effect to occur, the situation is the reverse. Inhibition of an enzymatic pathway involved in the bioactivation of a pro-drug, can result in decreased pharmacological effect.

CYP inhibition can be reversible, quasi-irreversible or irreversible [52, 54, 61, 63]. Reversible inhibition is the most common type of inhibition, and it occurs rapidly and causes only a transient loss in enzyme activity. Reversible inhibitors can be further categorized as competitive, noncompetitive, uncompetitive, and mixed type inhibitors [52, 54, 62-63]. In terms of drug metabolism, competitive inhibition is probably the most important mechanism and can be explained by structural similarities between the inhibitor and the substrate, which then compete for the active site of the enzyme. In noncompetitive and uncompetitive inhibition, the inhibitor and the substrate do not share the same binding site. Both mechanisms involve the formation of a nonproductive enzyme-substrate-inhibitor complex, with the difference that uncompetitive inhibitors do not bind to the free enzyme but only to the enzyme-substrate complex. The last, and frequently observed, class of reversible inhibitors is mixed type inhibitors, which exhibits elements of both competitive and noncompetitive inhibition. Here, the inhibitor and the substrate bind to different sites of the enzyme and the binding of one affects the binding for the other. In contrast to reversible inhibition, quasi-irreversible and irreversible inhibitions cause a permanent loss in enzyme activity. Both types require at least one catalytic cycle of the CYP enzyme, resulting in the formation of reactive metabolites that *in vivo*

irreversibly inactivate the enzyme. Irreversible inhibitors are often referred to as mechanism-based inactivators because metabolic activation is required for enzyme inhibition to occur [52, 54, 63]. Typical characteristics of mechanism-based inhibition are the time-, concentration-, and NADPH-dependent loss in enzyme activity [54]. The time-dependent phenomenon is the most important criteria in distinguishing between reversible and irreversible inhibition. Generally, mechanism-based inactivators cause a more profound effect compared to reversible inhibitors, and the inhibitory effect can be regained only by the synthesis of new, functional enzymes. However, mechanism-based inhibition is generally considered to be relatively unusual.

Induction of CYP enzymes

Drug interaction can also be a consequence of CYP induction following prolonged administration of drugs. In contrast to inhibition, enzyme induction is a slow regulatory process with a time-dependent increase in enzyme activity in response to an enzyme inducing agent [62]. The increase in CYP activity is a consequence of elevated levels of the induced protein [63]. Most often this is due to transcriptional activation, which to a large extent is mediated by ligand-activated transcription factors. These intracellular receptors include, for example, aryl hydrocarbon receptor (AhR), which mainly controls the induction of the CYP1 family, and pregnane X receptor (PXR), constitutive androstane receptor (CAR), and peroxisome proliferator-activated receptor (PPAR), which all are important for induction of the hepatic CYP2 and CYP3 families [54, 63]. Some nontranscriptional mechanisms are also known to be involved in CYP induction, including a decrease in the rate of protein degradation and stabilization of the protein. This may increase the CYP concentrations more rapidly than after induction due exclusively to transcriptional activity. A major concern related to CYP induction is a reduction in pharmacological effect due to increased drug metabolism [62-63]. However, in the case of a pro-drug, the effect is the reverse, with an increase in pharmacological effect as the biologically active metabolite is formed to a larger extent. CYP induction may also have toxicological implications if chemically reactive metabolites are formed that can react covalently with cellular macromolecules and cause increased toxicity [62].

If a drug induces enzymes that are involved in its own metabolism, this is called *autoinduction*. As a consequence, the metabolic clearance of the drug will increase over time, resulting in a time-dependent decrease in drug exposure. Remarkable time-dependency in the pharmacokinetics of artemisinin has been observed [64-66], attributed to autoinduction of CYP2B6 [67]. A proposed mechanism is the activation of CAR and PXR by

artemisinin, resulting in increased CYP2B6 mRNA expression [68], as schematically explained in Fig. 4.

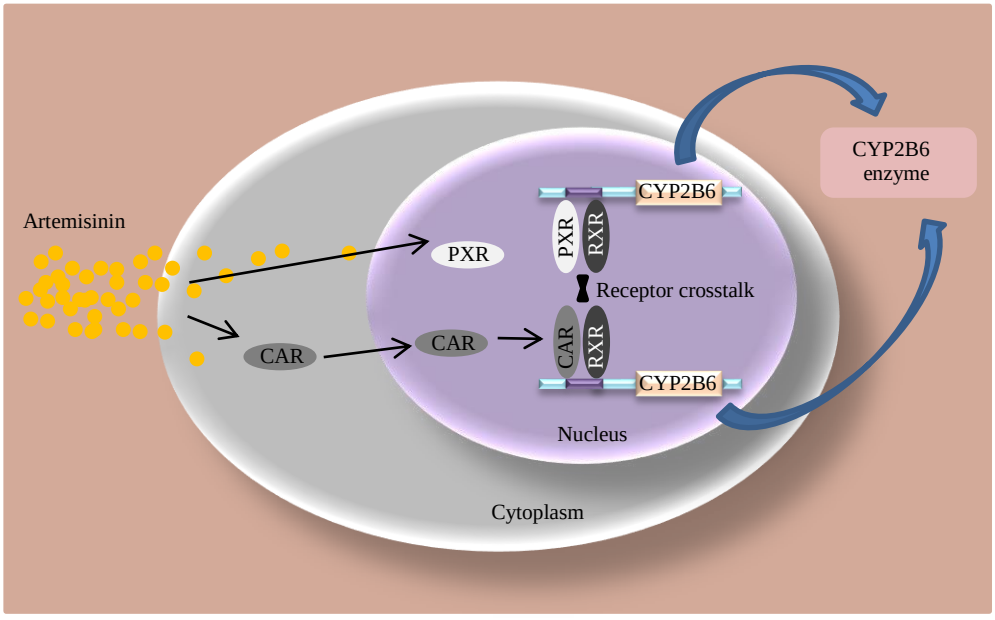

Figure 4. Artemisinin-mediated activation of the CYP2B6 gene by CAR and PXR. Artemisinin binds to endogenous CAR in the cytoplasm, which initiate the translocation of CAR into the nucleus. PXR on the other hand resides within the nucleus, and the artemisinin-mediated activation occurs here. Both CAR and PXR interact with the orphan retinoid X receptor (RXR), and the respective heterodimer binds to specific binding sites in promoter and enhancer regions of the CYP2B6 gene, resulting in induced transcription and synthesis of new CYP2B6 protein [68].

1.2.3 *In vitro* methods for CYP inhibition

In order to understand a potential enzyme inhibition and DDI *in vivo*, findings from *in vitro* interaction studies are valuable. Microsomes with cDNA-expressed metabolic enzymes and human liver microsomes (HLM) are two well accepted experimental systems widely used for screening of *in vitro* inhibitory potency of drugs [61, 69-70]. The recombinant expressed human CYP enzymes represent the simplest *in vitro* model, and it allows the investigation of the activity of specific enzymes separately. HLM consists of vesicles of the hepatocyte endoplasmic reticulum containing CYP and UDP-

glucuronosyltransferase (UGT) enzymes, and it offers the advantage of testing multiple enzymes simultaneously in one assay. The general experimental approach to assess potential CYP inhibition (or activation) *in vitro* is schematically described in Fig. 5. It includes incubations with recombinant CYPs or HLM, selective CYP probe substrates, co-factor to enable the catalyzed reaction, and the test compound to be evaluated for inhibition. The principle is to use probe substrate(s) specific for the CYP enzyme(s) to be investigated. The substrate is metabolized by the CYP enzyme to a product (metabolite), which can be measured by using, for example, fluorometric or liquid-chromatgraphy-mass spectrometry (LC-MS) assays. In the presence of an inhibitory test compound, the metabolite formation will be decreased or prevented compared to uninhibited controls.

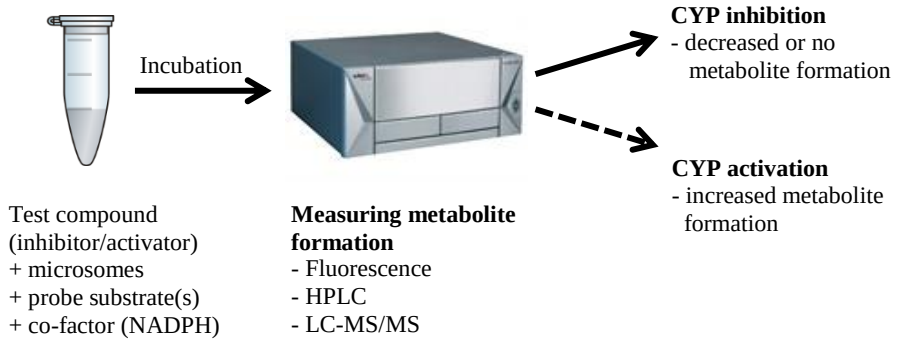

Figure 5. General experimental approach for the assessment of CYP inhibition (and activation) in vitro.

1.2.4 *In vitro–in vivo* extrapolation

The usefulness of *in vitro* data to predict the risk of metabolic DDIs *in vivo* is well accepted. *In vitro-in vivo* extrapolation (IVIVE) can be based on the two parameters, K_i (inhibition constant) and [I] (inhibitor concentration available to the enzyme *in vivo*), in order to quantitatively predict the degree of interaction *in vivo*. This can be achieved by calculating the ratio between the area under the plasma concentration-time curve (AUC) for the inhibited state (AUC_i) and the uninhibited control state, as described by Equation 1 [71-72]:

$$\frac{AUC_i}{AUC} = 1 + \frac{[I]}{K_i} \quad \text{(Eq. 1)}$$

An AUC ratio below 1.1 indicate a low risk of DDIs *in vivo*, ratios between 1.1 and 2 indicate a medium risk, while an inhibitor that increase the ratio >2 poses a high risk of causing a significant interaction *in vivo*. However, using *in vitro* data to predict the outcome *in vivo* always involves a degree of uncertainty. Design of *in vitro* assays to assess K_i, and the selection of inhibitor concentrations *in vivo* could have a major impact on the predicted *in vivo* interaction. Several other factors, such as the contribution of hepatic clearance to total clearance (f_H), fraction of metabolic clearance which is subject to inhibition (f_m), and route of administration, also affect the change in AUC ratio and the degree of interaction *in vivo*.

1.3 Drug concentration monitoring

The use of drug concentration monitoring in biological fluids is a necessity in pharmacokinetic studies, with plasma being the most widely used biological matrix [73-74]. However, the collection of blood is associated with discomfort for study participants and is not always the most desirable way of sampling. Saliva offers an easily accessible body fluid that can be sampled noninvasively without requiring special equipment or trained staff [74]. Therefore, saliva may be a more suitable alternative to plasma in drug monitoring and pharmacokinetic investigations where multiple sampling is needed.

The primary mechanism by which most drugs enter saliva is passive diffusion, a mechanism that allows only unbound and unionized fraction of drug in plasma to pass [73-75]. However, drug availability in saliva depends on multiple factors, including physiochemical properties of the drug (e.g. molecular size, lipophilicity, pK_a, protein binding), and physiological factors such as salivary pH and flow rate. Several studies have shown a proportional relationship between drug concentrations in saliva and plasma [76-79]. It is now accepted that for many drugs, salivary concentrations reflect unbound drug concentrations in plasma [73, 75]. For such drugs, saliva levels may be more reflective of drug concentrations at the site of action than total drug concentrations in plasma. Ideally, a drug that exhibits a constant saliva/plasma ratio and is consistent over concentration and time, would allow salivary concentrations to predict unbound plasma concentrations [75].

Distribution of artemisinin into saliva has been investigated, demonstrating high correlation between salivary and plasma concentrations [80-81]. In a pilot study with four healthy subjects, receiving a single artemisinin dose, saliva levels of artemisinin were closely related with unbound plasma concentrations [80]. The artemisinin saliva/plasma ratio was stabilized after a 3-hour period, and independent of both drug concentration and time thereafter. In another study with eighteen Vietnamese malaria patients receiving either 100 mg or 500 mg oral artemisinin doses, salivary concentrations of artemisinin were comparable to its unbound levels in plasma [81]. Together, these results suggest the use of saliva as a substitute to venous blood sampling in drug monitoring of artemisinin. Whether this is an alternative in the monitoring of ARS and DHA remains to be explored. Until now, no information regarding the distribution of these two compounds into saliva has been reported.

1.4 Bioanalytical method validation

Drug concentration monitoring in biological fluids requires selective and sensitive analytical methods for the quantification of drugs and their metabolites. Especially when using saliva as sampling matrix, higher demands are placed on assay sensitivity, since only unbound drug concentrations are being measured. The most commonly used technology is liquid chromatography coupled to tandem mass spectrometry (LC-MS/MS) [82]. To ensure reliability and reproducibility of a bioanalytical method developed for the analysis of clinical samples, regulatory authorities require the assay to be validated [83]. Bioanalytical method validation covers the assessment of fundamental parameters, including accuracy, precision, selectivity, sensitivity, reproducibility, and stability of the analytes [82-83].

Accuracy and precision

Accuracy accounts for the degree of closeness of mean test measurements obtained by the method to the actual (true) concentration of the analyte. It is determined by the relative error (%RE). Precision describes the degree to which repeated measures of an analyte show the same result under unchanged conditions, and is presented by the coefficient of variation (CV). Intra- and inter-run accuracy and precision should be established by replicate ($n \geq 5$) analysis of at least three concentrations (low, mid, and high). Acceptable limits for accuracy and precision are 85-115% (±15%) and <15%, respectively, except at the lowest measurable concentration (see LLOQ below).

Selectivity

High selectivity of an assay ensures the quantification of the intended analytes in presence of endogenous matrix components, known metabolites, degradation products or concomitant medication.

Sensitivity

This parameter is defined as the lower limit of quantification (LLOQ), which represent the lowest concentration of the analyte that can be measured with acceptable accuracy (RE< ±20%) and precision (CV<20%).

Reproducibility

This parameter is related to precision, and accounts for the precision of the analytical method over time (inter-day precision), given the same operating conditions. It can also represent the precision between different laboratories.

Stability

Evaluation of the stability of the test compounds is critical during the validation process to ensure the integrity of study data. Stability testing should be performed using experimental conditions that reflect actual situations encountered during sample handling and analysis. Current guidance requires the assessment of freez-thaw stability, short-term temperature and long-term stability, post-preparative stability (e.g. autosampler stability), and stock solution stability.

Another important parameter to consider during the validation process is *recovery*, which refers to the extraction efficiency of the assay during the work up procedure. In this experiment the detector response of an analyte from an extracted sample will be compared to the analytical response of an unextracted sample, which will represent 100% recovery. There is no absolute requirement for an analytical method to exhibit very high recovery, but the outcome should be consistent, precise, and reproducible [82-83].

1.5 Pharmacometrics

Pharmacometrics is a relatively new discipline, but with a growing importance in drug development. It has been described by Williams and Ette, who defined pharmacometrics as “the science of developing and applying mathematical and statistical models to: (a) characterize, understand, and

predict a drug´s pharmacokinetic, pharmacodynamic, and bio-marker outcomes behavior, (b) quantify uncertainty of information about that behavior, and (c) rationalize data-driven decision making in the drug development process and pharmacotherapy" [84]. To understand and quantify beneficial and adverse outcomes of drugs in patients, mathematical models of biology, pharmacology, disease, and physiology are applied. Pharmacometrics is a bridging discipline associated with related disciplines such as basic and clinical pharmacology, biostatistics and medicine. Within the pharmaceutical industry, population pharmacokinetic analysis is perhaps the most commonly applied type of pharmacometric modelling, and regulatory guidelines for this have been developed and published [85].

1.5.1 Population pharmacokinetics

Population pharmacokinetics is the study of pharmacokinetics at the population level [4]. It allows the use of relatively sparse data obtained from study subjects, but also of dense data or a combination of dense and sparse data. One of the primary goals with population pharmacokinetic analysis is to estimate population pharmacokinetic parameters and variability observed in these parameters. It also seeks to identify patient characteristics, so-called covariates, that could explain the variability in drug pharmacokinetics or pharmacodynamics and drug exposure [3-4]. Population parameters include *fixed effect* parameters and *random effect* parameters. Fixed effect parameters define the average value of a pharmacokinetic parameter (e.g. clearance and volume of distribution) in a population and/or the relationship between covariates and pharmacokinetic parameters. Random effect parameters quantify the unexplained random variability, including the between-subject variability (BSV) and residual (unknown) variability [86]. The most commonly applied method in population pharmacokinetics is the nonlinear mixed-effects modelling approach. One common program for population pharmacokinetic analysis is NONMEM (ICON Development Solutions, Ellicott City, MD, USA) developed by Beal and Sheiner [87].

1.5.2 Nonlinear mixed-effects modelling

Nonlinear mixed-effects modelling enables pooled data from all individuals in a study population to be evaluated, allowing all fixed effect and random effect parameters to be estimated and quantified simultaneously [4, 86]. The term "nonlinear" refers to the nonlinear relationship between the dependent variable (e.g. concentration) and the model parameters and independent variable(s). As seen in Fig. 6, nonlinear mixed-effects population pharmacokinetic models are comprised of several components for the

estimation of all types of population parameters: (1) structural model, (2) statistical model, and (3) covariate model [3-4, 86].

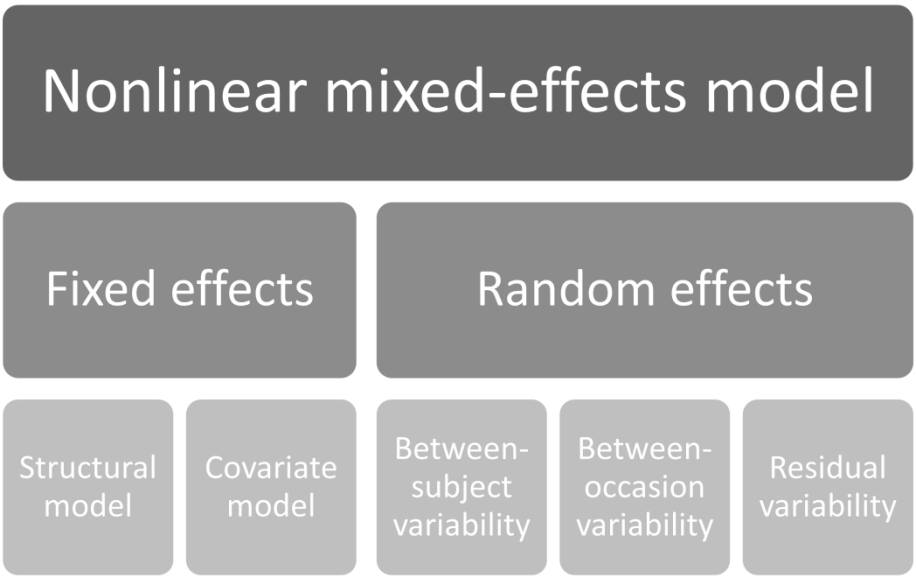

Figure 6. Schematic picture of a nonlinear mixed-effects model and its components. Adapted from Rekić, D., Quantitative Clinical Pharmacological Studies on Efavirenz and Atazanavir in The Treatment of HIV-1 Infection (ISBN 978-91-628-8590-8)

The *structural model* includes a pharmacokinetic model, describing the typical concentration-time data within the population. The simplest form is a one-compartment distribution model with first-order elimination following a single intravenous bolus dose, which could be represented by the algebraic Equation 2:

$$C_p = \frac{Dose_{\ iv}}{V} \cdot e^{\left(-\frac{CL}{V} \cdot t\right)} \qquad \text{(Eq. 2)}$$

where C_p represents the predicted plasma drug concentration at time point, t, after the given dose ($Dose_{iv}$), based on the volume of distribution (V) and elimination clearance (CL).

The *statistical model* aims to describe the unexplained (random) variability in the observed data, including BSV and residual variability. BSV refers to the

random variability between individuals, and can be described by the Equation 3:

$$P_i = \theta_{pop} \cdot e^{\eta_{i,p}} \quad \text{(Eq. 3)}$$

where P_i is the estimated parameter value for the i^{th} individual, θ_{pop} represents the population mean of parameter P and $\eta_{i,P}$ is the deviation of P_i from θ_{pop}, and accounts for the individual difference from the typical estimate. BSV is estimated from a normal distribution with zero mean and variance ω^2, however, this assumption is not always correct. [4]. When all other sources of variability have been accounted for, the remaining unexplained variability is referred to as residual variability. It includes, among other things, measurements and assay variability error, errors in the recorded time of sampling, and any model misspecification error. The residual error model quantifies the remaining difference between the individual predicted concentrations ($C_{pred,ij}$) and individual observed concentrations (C_{ij}). Using log-transformed data and an additive residual error model (essentially equivalent to an exponential error model on an arithmetic scale), the variability could be described by Equation 4:

$$\ln C_{ij} = \ln C_{pred,ij} + \varepsilon_{ij} \quad \text{(Eq. 4)}$$

where C_{ij} represents the j^{th} observation for individual i, $C_{pred,ij}$ represents the j^{th} predicted drug concentration for individual i, and ε_{ij} represents the residual random error for the j^{th} observation of individual i. The term ε is assumed to be normally distributed with a mean of zero and a variance σ^2. [3-4, 86].

The *covariate model* includes subject specific characteristics (covariates), which are used to describe predictable sources of variability [3-4, 86]. Modelling covariates aims to identify and explain parts of the BSV and predict subject specific differences. Covariates could be classified as continuous (e.g. body weight, age, renal and hepatic function) or categorical (e.g. sex, ethnicity) covariates. The relationship between covariates and model parameters can be explained by, for example, linear, exponential, power or proportional functions. Using a linear function, the effect of a continuous covariate on a parameter could be explained by Equation 5:

$$P_i = \theta_{pop} \cdot \left(1 + \theta_1 \cdot (COV - COV_{median})\right) \quad \text{(Eq. 5)}$$

where COV being the continuous covariate centered to the population median (COV_{median}), and θ_1 is a factor describing the correlation between the covariate and the parameter.

2 AIM

The two primary aims with this thesis were (1) to investigate the effect of artemisinin endoperoxides on the activity of human liver Cytochrome P450 enzymes *in vitro*, and (2) to study the pharmacokinetics of ARS, as the drug orally administrated, and its active metabolite DHA in plasma and saliva during long-term treatment in patients with breast cancer by developing a highly sensitive LC-MS analytical method. The specific aims addressed in each paper were:

1. To investigate the effect, and its possible time-dependency, of artemisinin endoperoxides on CYP2B6 *in vitro*, and to extrapolate the results to assess the risk of interaction *in vivo*. **(Paper I)**

2. To investigate the effect of artemisinin endoperoxides on seven of the major human liver CYP enzymes (CYP1A2, 2A6, 2B6, 2C9, 2C19, 2D6 and 3A4) *in vitro*. **(Paper II)**

3. To develop and validate a bioanalytical assay based on solid phase extraction and LC-MS/MS detection for the quantification of administrated ARS and its active metabolite DHA in human plasma and saliva. **(Paper III)**

4. To study the pharmacokinetics of ARS and DHA in patients with breast cancer, using non-compartmental analysis. **(Paper IV)**

5. To characterize the population pharmacokinetics of ARS and DHA during long-term oral ARS treatment in patients with breast cancer, and to investigate the correlation between salivary and plasma concentrations, using nonlinear mixed-effects modelling. **(Paper V)**

3 METHODS

3.1 Paper I and II – CYP inhibition studies

3.1.1 Recombinant enzyme incubations

Recombinant expressed human CYP enzymes (rCYP) were used to investigate the activity of specific enzymes separately. All incubations were conducted in microtiter plates at 37°C with a final working volume of 200 µL/well. Test artemisinin endoperoxides (single or multiple concentrations), positive controls or vehicle in buffer (phosphate buffer or Tris buffer, pH 7.4, depending on rCYP isoform, see Table 1) were pre-incubated (37°C) for 10 min in the presence of a NADPH-regenerating system (1.3 mM $NADP^+$, 3.3 mM G-6-P, 3.3 mM $MgCl_2$ and 0.4 U/mL G-6-P-D for rCYP1A2, 2B6, 2C9 and 2D6; 8.2 µM $NADP^+$, 0.41 mM G-6-P, 0.14 mM $MgCl_2$ and 0.4 U/mL G-6-P-D for rCYP2A6, 2C19 and 3A4). In the time-dependent inhibition (TDI) assay (Paper I), incubations were also conducted in the absence of NADPH to investigate potential time-dependency of the artemisinin mediated inhibition. Reactions were initiated by the addition of a solution containing the respective rCYP and selected pro-fluorescent substrate (Table 1). Reactions were allowed to run for an appropriate incubation time before terminated by the addition of 75 µL stop solution (20% Tris base/80% acetonitrile). Fluorescence was measured using a Tecan Infinite F200 fluorometer (Tecan Nordic AB, Mölndal, Sweden). The intensity of the response was used as a measure of the formation rate of fluorescent metabolite. The percentage activity remaining was calculated by comparing the inhibited activity (fluorescence intensity) with non-inhibited controls.

3.1.2 Microsomal incubations

Efavirenz 8-hydroxylation assay (Paper I)

To assess the enzymatic activity of microsomal CYP2B6, the formation of 8-hydroxyefavirenz from efavirenz was measured. All incubations were conducted in 2 mL Eppendorf tubes at 37°C with a final working volume of 500 µL/tube. Efavirenz (single or multiple concentrations) was incubated with HLM (0.25 mg protein/mL) and a NADPH-regenerating system (1.3 mM $NADP^+$, 3.3 mM G-6-P, 3.3 mM $MgCl_2$ and 0.4 U/mL G-6-P-D) in the absence and presence of artemisinin test compounds (single or multiple concentrations) or in the presence of positive control (ticlopidine). Reactions were allowed to run for 30 min before terminated by the addition of 500 µL acetonitrile containing internal standard (nevirapine, 15 µM). After

centrifugation (14 000 *g* for 10 min at 4°C) the supernatant was transferred to clean tubes and extracted twice with ethyl acetate under alkaline pH as described previously [55]. The organic phase was transferred to clean tubes, evaporated to dryness, and the residue was reconstituted with 100 µL of mobile phase.

Cocktail incubation (Paper II)

To assess the enzymatic activity of microsomal CYP1A2, 2A6, 2B6, 2C9, 2C19, 2D6 and 3A4, a previous described assay was adopted and modified [88]. All incubations were conducted in a 96-well plate format at 37°C with a final working volume of 200 µL/well. Test artemisinin compound (single or multiple concentrations) positive controls or vehicle in phosphate buffer were pre-incubated (37°C) for 10 min in the presence of a NADPH-regenerating system (1.3 mM $NADP^+$, 3.3 mM G-6-P, 3.3 mM $MgCl_2$ and 0.4 U/mL G-6-P-D). Reactions were initiated by the addition of a solution containing HLM (0.25 mg protein/mL) and substrates (divided into set A and B, see Table 2). Reactions were allowed to run for 20 min before placed on ice and terminated by the addition of 200 µL cold acetonitrile containing internal standard (chlorpropamide, 20 µM). After centrifugation (3000 *g* for 20 min in room temperature) supernatants from set A and B were pooled together and analyzed by LC-MS/MS.

3.1.3 Analytical methods

High-performance liquid chromatography (HPLC) for quantification of 8-hydroxyefavirenz (Paper I)

A previously described HPLC assay with UV detection was adopted and modified for the quantification of efavirenz and 8-hydroxyefavirenz. The HPLC system consisted of an Agilent 1260 Infinity pump and autosampler, connected to an UV detector set at 247 nm for the monitoring of analytes. Separation of efavirenz, 8-hydroxyefavirenz and internal standard was achieved using a Phenomenex (Torrance, CA) Kinetex C_{18} column (100 x 4.6 mm; 2.6 µM). A total run time of 9 min (plus 8 min wash out period with acetonitrile) with an isocratic flow rate of 0.3 mL/min and a mobile phase consisting of acetonitrile and 0.1% formic acid (55:45; v/v) resulted in good separation of the analytes. Data acquisition and integration of analyte peaks were performed using the Clarity chromatography software (DataApex, The Czech Republic). The percentage activity remaining was calculated by comparing the formation rate of 8-hydroxyefavirenz in each sample relative to the average metabolite formation rate of non-inhibited controls.

LC-MS/MS method for cocktail incubations (Paper II)

Quantification of all formed metabolites in the HLM cocktail incubations were achieved using an API 3000 triple quadropole mass spectrometer (Applied Biosystems/MDS SCIEX, Foster City, CA) connected to an autoinjector and two pumps in the Perkin Elmer 200 Series (Perkin Elmer, Waltham, MA). Mass spectrometric conditions were optimized for each metabolite, using electrospray ionization (ESI) and a positive ion mode, with ESI voltage set to 5000 V and ESI temperature maintained at 400^{o}C. High purity nitrogen was used as nebulizer gas (9 psi), curtain gas (6 psi) and collision gas (8 psi). Multiple reaction monitoring (MRM) was used to quantify the metabolites, and final MRM transitions (*m/z*) are presented in Table 2.

Separation of analytes was achieved using a Luna C_{18} column (30 x 2.0 mm; 5 µm) (Phenomenex, Torrance) protected by a C_{18} guard cartridge (4.0 x 3.0 mm) (Phenomenex ApS, DK). The mobile phase consisted of 0.1% formic acid in water (A) and 0.1% formic acid in acetonitrile (B). A gradient flow (0.2 mL/min) was applied, with mobile phase B linearly increasing from 10% to 80% during 1 min, held at 80% for an additional 2 min and then linearly decreasing to 10% over 30 sec for re-equilibration (total run time 6.5 min). Data acquisition and integration of analyte peaks were performed using Analyst 1.4 (Applied Biosystem/MDS SCIEX, Foster City, CA). The percentage activity remaining was calculated by comparing the substrate metabolite concentrations of inhibited samples relative to the average substrate metabolite concentrations of non-inhibited controls.

LC-MS/MS method for 4´-hydroxymephenytoin (Paper II)

An API 4000 triple quadropole mass spectrometer (Applied Biosystems/MDS SCIEX, Foster City, CA) connected to a CTC PAL autosampler (Leap Technologies, Carrboro, NC) and two Perkin Elmer 200 Series pumps were used to quantitate low concentration of 4´-hydroxymephenytoin in the HLM cocktail incubations. Mass spectrometric conditions were optimized for the metabolite and the internal standard, using ESI and a positive ion mode, with ESI voltage set to 5500 V and ESI temperature maintained at 225^{o}C. Collision gas was set to 12 psi, curtain gas to 17 psi, and ion source gas one and two to 12 and 19 psi, respectively. Final MRM transitions (*m/z*) are presented in Table 2.

The same HPLC columns and mobile phase as described for the overall cocktail incubations were used. A gradient flow (0.2 mL/min) was applied,

with mobile phase B held at 25% during 1.5 min, before linearly increasing to 95% over 0.1 min, and held at this value for an additional 1.5 min, before finally linearly decreasing to 25% over 0.1 min for re-equilibration (total run time 5.5 min). During the first 0.6 min after injection, the LC eluent was diverted to waste to minimize contamination of the ion source. Data acquisition and integration of analyte peaks were performed using Analyst 1.4 (Applied Biosystem/MDS SCIEX, Foster City, CA). The percentage activity remaining was calculated by comparing the analyte peak area/IS peak area ratio of inhibited samples with the analyte peak area/IS peak area ratio of non-inhibited controls.

Table 1. Experimental conditions for the fluorometric assay using rCYP.

P450 isoform	**Substrate**	**Metabolite**	**Buffer (mM)**
1A2	CEC	CHC	KPO_4 (100)
2A6	COU	HC	Tris (100)
2B6	EFC	HFC	KPO_4 (100)
2C9	MFC	HFC	KPO_4 (25)
2C19	CEC	CHC	KPO_4 (50)
2D6	AMMC	AMHC	KPO_4 (100)
3A4	BFC	HFC	KPO_4 (200)
3A4	DBF	Fluorescein	KPO_4 (200)

Abbreviations: AMMC, 3-[2-(N,N-diethyl-N-methylammonium)-ethyl]-7-methoxy-4-methylcoumarin; BFC, 7-benzyloxy-4-trifluoromethylcoumarin; CEC, 7-ethoxy-3-cyanocoumarin; COU, coumarin; DBF, dibenzylfluorescein; EFC, 7-ethoxy-4-trifluoromethylcoumarin; MFC, 7-methoxy-4-trifluoromethylcoumarin; AMHC, 3-[2-(N,N-diethyl-N-methylammonium)ethyl]-7-hydroxy-4-methylcoumarin; HFC, 7-hydroxy-4-trifluoro-methylcoumarin; CHC, 7-hydroxy-3-cyanocoumarin; HC, 7-hydroxycoumarin.

Table 2. Experimental conditions and MRM parameters for the P450 probe substrates and internal standard (IS) used in the cocktail assay.

P450 isoform	Substrate	Metabolite	Transition (*m/z*)
1A2	Phenacetin[a]	Acetaminophen	152 > 120
2A6	Coumarin[a]	7-Hydroxycoumarin	163 > 107
2B6	Bupropion[b]	Hydroxybupropion	256 > 238
2C9	Tolbutamide[b]	4-Hydroxytolbutamide	287 > 89
2C19	S-Mephenytoin[a]	4´-Hydroxymephenytoin	235 > 150
2D6	Dextromethorphan[a]	Dextrorphan	258 > 157
3A4	Midazolam[a]	1-Hydroxymidazolam	342 > 203
IS	Chlorpropamide		277 > 175

[a] Substrate set A
[b] Substrate set B

3.1.4 Data analysis

IC_{50} determinations

IC_{50} values were estimated by fitting an inhibitory effect I_{max} model (Equation 6; gamma fixed to 1) or an inhibitory effect sigmoid I_{max} model (Equation 6; gamma estimated) to unweighted data using Phoenix®WinNonlin® 6.2 (Pharsight Corp, Mountain View, CA).

$$\%\ Remaining\ activity = E_0 - \frac{I_{max} \cdot [I]^{\gamma}}{IC_{50} + [I]^{\gamma}} \qquad \text{(Eq. 6)}$$

where E_0 represents maximal enzyme activity in the absence of inhibitor, I_{max} is the maximum drug induced inhibition of the enzyme activity, [I] is the concentration of the inhibitory drug, and γ describes the sigmoidicity of the relationship. Model discrimination was based on evaluation of parameter estimate precisions (relative standard errors), correlation between observed and predicted variable values, residual plots and the Akaike information criterion (AIC).

Determination of inhibition mechanism and K_i in rCYP

To evaluate the mechanism of rCYP inhibition, apparent V_{max} and K_m values in the absence and presence of inhibitor were estimated. This was achieved by fitting a single site Michaelis-Menten equation, $V = (V_{max} \times [S])/(K_m + [S])$, to metabolite formation (fluorescence intensity) of control and inhibited samples versus substrate concentrations, using Sigma Plot 2001, Enzyme Kinetics Module 1.1 (SPSS Science Ltd, Birmingham, UK). Further, enzyme kinetic parameters (K_m, V_{max}, and K_i) were estimated by simultaneously fitting eight kinetic equations, describing different mechanisms of inhibition, to metabolite formation (fluorescence intensity) in absence and presence of increasing concentrations of inhibitor versus substrate concentrations, using the same software.

Predicted change in drug exposure in vivo

IVIVE using the $[I]/K_i$ ratio as previously explained by Equation 1 (see section 1.2.4), was applied to evaluate the clinical relevance of a potential enzyme inhibition. The maximum unbound systemic concentrations of the inhibitor ($[I]_{max,u}$) and the maximum unbound concentrations of the inhibitor at the inlet to the liver ($[I]_{max,inlet,u}$; calculated as proposed by Ito *et al*. [89]) were calculated and used.

Time-dependent inhibition (Paper I)

To evaluate potential time-dependency of the artemisinin induced inhibition on CYP2B6 activity, IC_{50} values were estimated after 15 and 30 min incubations respectively. Further, TDI ratios for low (5 µM) and high (50 µM) concentrations of artemisinin were calculated according to Equation 7:

$$TDI\ ratio\ = \frac{(R+I^{NADPH})/(R-I^{NADPH})}{(R+I^{noNADPH})/(R-I^{noNADPH})} \qquad \text{(Eq. 7)}$$

$R\text{-}I^{NADPH}$ is the rate of reaction (fluorescence intensity) when pre-incubation is performed in the presence of NADPH but in the absence of inhibitor and represents the activity of uninhibited enzyme (100% activity). $R+I^{NADPH}$ is the rate of reaction when pre-incubation is performed in the presence of both inhibitor and NADPH. This allows the formation of potentially reactive metabolites of the inhibitor, which is necessary in the case of mechanism-based inhibition. $R+I^{noNADPH}$ is the rate of reaction when pre-incubation is performed in the presence of inhibitor but in the absence of NADPH. In this reaction, no metabolites of the inhibitor can be formed, and therefore it caters

for the inhibitory effect due to modes other than mechanism-based inhibition. $R\text{-}I^{noNADPH}$ is the rate of reaction when pre-incubation is performed in the absence of both inhibitor and NADPH. This term is included to see if NADPH has any effect on the death of the enzyme, and to control for potential loss in enzyme activity when adding NADPH without any substrate. TDI ratios below 0.7-0.8, with the lower inhibitor concentration showing lower ratio compared to the higher concentration, are considered to be an indication of TDI, while ratios above 0.9 indicate non-TDI.

3.2 Paper III – Bioanalytical method for quantification of ARS and DHA in human plasma and saliva

3.2.1 Instrumentation

The LC-MS/MS system consisted of an API 3000 triple quadropole mass spectrometer (Applied Biosystems/MDS SCIEX), connected to a temperature-controlled autoinjector (set at 8°C) and a pump in the Perkin Elmer 200 Series (Perkin Elmer, Waltham, MA). The software Analyst 1.4.2 (AB Sciex, MA, US) was used for system control, data acquisition, and analyte quantification during bioanalysis.

3.2.2 Sample preparation and LC–MS/MS assay

Clinical plasma and saliva samples were processed and analyzed together with standards (ranging from 5 to 1000 ng/mL and 5 to 2000 ng/mL for ARS and DHA, respectively) and quality control (QC) samples. Samples preparation for the extraction of ARS, DHA and internal standard (IS, artemisinin) from the biological matrices included solid phase extraction (SPE), using a HyperSep Retain PEP (polar enhanced polymer) 96-well plate (Thermo Scientific, PA, USA).

Twenty microliters of the final SPE eluent was injected onto the LC-MS/MS system and analyzed on a BETASIL phenyl-hexyl column (50 x 2.1 mm; 5 µm) protected by a BETASIL phenyl-hexyl guard cartridge (10 x 2.1 mm; 5 µm). A total run time of 6 min with an isocratic flow rate of 0.2 mL/min and a mobile phase consisting of acetonitrile-ammonium acetate 10 mM pH 4.0 (50:50, v/v) were applied.

Mass spectrometric conditions had been optimized previously for the MRM analysis of ARS, DHA and IS. ESI and a positive ion mode were used with

the ESI temperature maintained at 225°C and the ESI voltage set to 5500V. Nebulizer, curtain, and collision gas were optimized to 15, 10, and 4 psi, respectively. Compound specific parameters are summarized in Table 3.

Table 3. Compound specific mass spectrometric parameters for ARS, DHA and IS.

	Transition (*m/z*)	**DP (V)**	**FP (V)**	**CP (V)**	**CXP (V)**	**EP (V)**
ARS	402.5-267.1	10	60	14	6	5
DHA	302.4-267.3	9	70	12	6	5
IS	300.4-209.2	15	65	15	4	5

Abbreviations: DP, declustering potential; FP, focusing potential; CP, collision potential; CXP, collision exit potential; EP, entrance potential; IS, internal standard

3.2.3 Method validation

The LC-MS/MS method was validated according to Food and Drug Administration (FDA) guidelines [83]. The validation was carried out in terms of selectivity, sensitivity, accuracy, precision, recovery, and stability, as explained in section 1.4.

3.2.4 Application to clinical plasma and saliva samples

The method was implemented for the quantification of ARS and DHA in plasma and saliva samples obtained in a clinical study with ARS given to patients with breast cancer (study design described in section 3.3.1). Blood and saliva samples were collected at time points 0, 0.25, 0.5, 0.75, 1, 1.25, 1.5, 2, 3, 4, 6 and 8 hours post-dose. All samples were processed and stored in -75°C as described in section 3.3.1, until analyzed by the presented method.

3.3 Paper IV – Pharmacokinetics of ARS and DHA in patients with breast cancer

3.3.1 Study design

The present work includes data from patients with metastatic breast cancer, enrolled in a pharmacokinetic substudy to the ARTIC study. The main study is a prospective open, uncontrolled, monocentric tolerability study conducted at the Medical Clinic at the University of Heidelberg, Germany (ClinicalTrials.gov NCT00764036). The study protocol was approved by the competent authority (Federal Institute of Drugs and Medical Devices

(BfArM), EudraCT 2007-004432-23) and the ethics committee of the Medical Faculty of Heidelberg (ref.: AFmu495/2007). All patients provided a signed written informed consent prior to enrolment.

23 patients were enrolled in the main study and allocated into three different study arms in a dose escalating manner (100 mg, 150 mg or 200 mg oral ARS once daily). Pharmacokinetic sampling from patients participating in the substudy was conducted on the first day of medication for the evaluation of single dose kinetics, and after three weeks of daily medication for the evaluation of steady state kinetics. Plasma and saliva samples were collected at time points 0, 0.25, 0.5, 0.75, 1, 1.25, 1.5, 2, 3, 4, 6 and 8 hours post-dose.

3.3.2 Pharmacokinetic analysis

Non-compartmental analysis (NCA) using the Kinetica 5.0 software (Thermo Kinetica Inc, CA, USA) was carried out for pharmacokinetic analysis for each dose group. Maximal drug concentration (C_{max}), time to reach maximal drug concentration (T_{max}), area under the curve (single dose: AUC_{total}, steady state: $AUC_{0\text{-}24h}$), and clearance (CL) were estimated for ARS and DHA, respectively. For the statistical comparison of estimated parameters after the first oral ARS dose and after at least three weeks of daily medication the paired t-test of log-transformed parameter values (for all but T_{max} and $t_{1/2}$) with a significance level of 0.05 was implemented in GraphPad Prism 5.01, (GraphPad Software Inc, CA, USA).

3.4 Paper V – Population pharmacokinetics of ARS and DHA in patients with breast cancer

3.4.1 Study design

The present work includes data from 23 patients with metastatic breast cancer, enrolled in the ARTIC study described in paper IV (section 3.3.1). The study was approved by the competent authorities (Federal Institute of Drugs and Medical Devices (BfArM), EudraCT 2007-004432-23) and the ethics committee of the Medical Faculty of Heidelberg (ref.: AFmu495/2007). All patients provided a signed written informed consent prior to enrolment.

Patients were divided into three different study arms, receiving 100 (n=6), 150 (n=7), or 200 mg (n=10) oral ARS once daily. Plasma and saliva samples

were collected at time points 0, 0.25, 0.5, 0.75, 1, 1.25, 1.5, 2, 3, 4, 6 and 8 hours post-dose after the first ARS administration as well as after a dose at least three weeks into the treatment. Additional sparse sampling was performed on an irregular basis, with plasma and saliva sampled 1-2 hours after ARS administration.

3.4.2 Model development

The ARS and DHA plasma and saliva concentrations were transformed into their natural logarithms. The M1, M3 and M6 methods were evaluated to account for observed data below the quantification limit (BQL). Using the M1 method, all BQL data was excluded and coded as missing data. In the M3 method, all BQL data was included and modeled as censored data using Laplacian estimation. Using the M6 method, only the first BQL value in a consecutive series was included (imputed as LLOQ/2), while all other values below the LLOQ were omitted.

The pharmacokinetic structural model for ARS and DHA was evaluated using full drug concentration-time profile plasma data and sparse sample plasma data. The two compounds were modelled simultaneously, assuming complete and irreversible conversion of ARS to DHA. ADVAN6 was applied for all modelling approaches. One- and two-compartment models with first-order absorption of ARS from the dose compartment were evaluated, with the assumption of first-order elimination from central compartment. The structural base model was parameterized as oral (for ARS) or apparent (for DHA) elimination clearance (CL/F), apparent volume of distribution of the central compartment (V_C/F), apparent intercompartmental clearance (Q/F) and apparent volume of distribution of the peripheral compartment (V_P/F). From here on, elimination clearance parameters will refer to oral elimination for ARS (CL_{ARS}/F) and apparent elimination for DHA (CL_{DHA}/F). A variety of absorption models were tested, as well as models describing partial pre-systemic conversion of ARS to DHA, and enterohepatic recirculation. BSV was initially investigated on all pharmacokinetic parameters, but only kept if they were estimated with reasonable precision and contributed to a sufficient reduction in the objective function value (OFV). Allometric scaling with body weight (BW) was evaluated on clearance parameters and apparent volumes of distribution, with pre-defined scaling factors fixed to 0.75 and 1 for clearance and volume, respectively. Using a stepwise approach with a forward addition ($p \leq 0.05$, $\Delta OFV > 3.84$) and a backward elimination ($p \leq 0.001$, $\Delta OFV > 10.83$) approach, the continuous covariates age, hemoglobin, and liver status (ALAT/ASAT) and their relationship with pharmacokinetic

parameters were evaluated according to Equation 5 (described in section 1.5.2).

Visual inspection of scatter plots indicated a reasonable good correlation between salivary and plasma DHA concentrations (Fig. 7). Using a predefined saliva/plasma concentration ratio of ≤0.5 as inclusion criteria, concentrations of DHA in saliva were incorporated in the final structural plasma model. Salivary DHA was proportionally scaled to plasma DHA, and all plasma and saliva data were fitted simultaneously (Equation 8):

$$DHA(S) = \theta_1 \cdot DHA(P) \qquad \text{(Eq. 8)}$$

where DHA concentrations in saliva are represented by DHA(S), total plasma concentrations of DHA by DHA(P), and θ_1 being the proportionality constant describing the relationship between DHA concentrations in saliva and plasma.

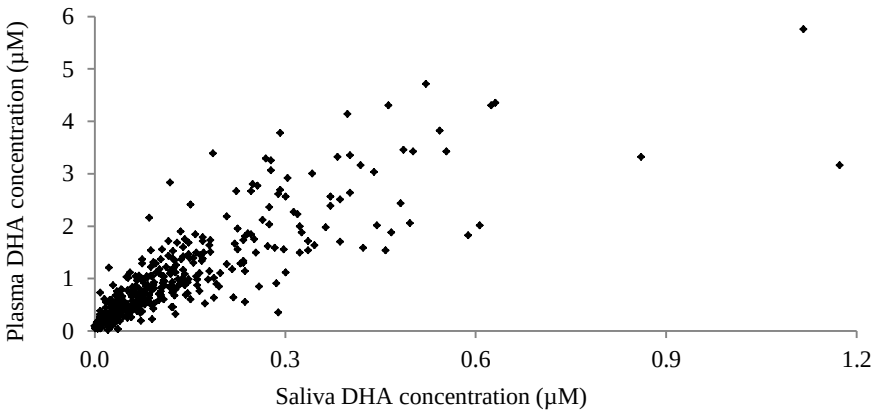

Figure 7. Observed concentrations of DHA in plasma versus observed DHA concentrations in saliva for all patients.

Using only full drug concentration-time profile plasma data from twenty-two patients, potential time-dependency in elimination clearance parameters of ARS and DHA was evaluated. Data represented two dose occasions; occasion 1 including full drug concentration-time profile data after the first oral ARS dose, and occasion 2 including full drug concentration-time profile data after a dose taken after at least three weeks daily medication). Using Equation 3

(described in section 1.5.2), elimination clearance for occasion 1 was estimated. To assess the time-dependent change in elimination clearance measured on occasion 2, Equation 9 was applied:

$$CL_i = \theta_{pop} \cdot (1 + \theta_1) \cdot e^{\eta_{i,P}} \quad \text{(Eq. 9)}$$

where θ_1 describes the relative change in clearance after at least three weeks daily ARS medication for the i^{th} individual with an estimated elimination clearance of CL_i.

3.4.3 Data analysis

The modelling software NONMEM version 7.1.2 (ICON Development Solutions, Ellicott City, MD, USA) was used in the population PK analysis, with the first-order conditional estimation (FOCE) method and the subroutine ADVAN6. Pearl-speaks-NONMEM (PsN, version 3.6.2) [90-91] and Xpose (version 4.0.4) [92] were used for data evaluation, graphics and handling of output files.

Throughout the model development, the change in OFV produced by the addition of a single model parameter (one degree of freedom) was used to evaluate the model appropriateness. OFV is proportional to minus twice the log-likelihood. With a chi-squared distribution, a decrease in OFV of 3.84 is approximately equivalent to a p-value of 0.05. Basic goodness-of-fit (GOF) plots and the precision of parameter estimates (expressed as relative standard error, %RSE) were also used to discriminate between models. Bootstrap diagnostics, stratified on ARS and DHA in each matrix, was used to generate %RSE and assess the precision of population parameter estimates. To assess the predictive performance of the models, visual predictive check (VPC) was performed using 1000 simulations at each concentration-time point. Simulated data were compared with observed data by calculating the 95% confidence interval (CI) around the simulated 5^{th}, 50^{th} and 95^{th} percentiles, and the same percentiles of observed data.

4 RESULTS

4.1 Paper I – CYP2B6 inhibition by artemisinin antimalarials *in vitro*

4.1.1 Recombinant CYP2B6 (rCYP2B6) activity

IC_{50}, K_i and mechanism of inhibition

The activity of rCYP2B6 was inhibited by artemisinin and ARM with estimated IC_{50} values of 9.50 ± 2.31 µM and 7.50 ± 0.88 µM, respectively. The inhibitory effects exerted by artemisinin (Fig. 8) and ARM (Fig. 9) were both best described by a partial mixed inhibition model (Equation 10), with decreasing apparent V_{max} values and increasing apparent K_m values with increasing inhibitor concentration (Fig. 10).

$$V = V_{max} \cdot \frac{\left(1+\frac{\beta \cdot I}{\alpha \cdot K_i}\right)\Big/\left(1+\frac{I}{\alpha \cdot K_i}\right)}{1+\left(\frac{K_m}{S}\cdot\left(1+\frac{I}{K_i}\right)\right)\Big/\left(1+\frac{I}{\alpha \cdot K_i}\right)} \qquad \text{(Eq. 10)}$$

where V represents the rate of metabolite formation, V_{max} the maximal rate of metabolite formation, S and I are the substrate and inhibitor concentrations, respectively, and K_m is the substrate affinity constant. The change in binding affinity in the presence of inhibitor is described by the term α, and the decrease in V_{max} for partial mixed inhibition is accounted for by the term β. Predicted K_i values based on Equation 10 were 3.64 ± 0.36 µM and 3.10 ± 0.29 µM for artemisinin and ARM, respectively.

DHA did not show any inhibitory effect on rCYP2B6 activity.

Time-dependent inhibition

The estimated IC_{50} value for artemisinin for 15-min incubation (10.3 ± 2.72 µM) did not differ markedly from the estimated IC_{50} value after 30 min incubation, indicating no time-dependency. This was further strengthened by the calculated TDI ratios, which was lower (0.95 ± 0.02) at a artemisinin concentration of 5 µM compared with at 50 µM (1.31 ± 0.23), indicating non-TDI.

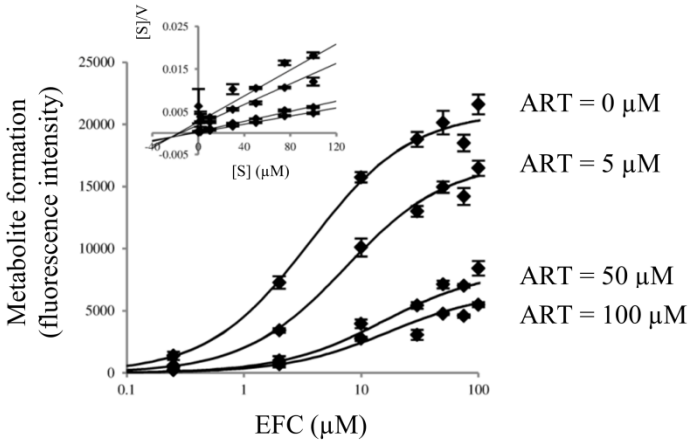

Figure 8. Observed (diamonds) and predicted (lines) formation of HFC, represented by the fluorescence intensity, from EFC (substrate, S) in rCYP2B6 in the absence and presence of varying concentrations of artemisinin (ART). Predictions were obtained by simultaneously fitting a partial mixed inhibition model to the pooled data. Observed data in the graph are presented as mean ± SE (n = 4). Inset: Hanes-Woolf plot for the inhibition of HFC formation in rCYP2B6 by artemisinin.

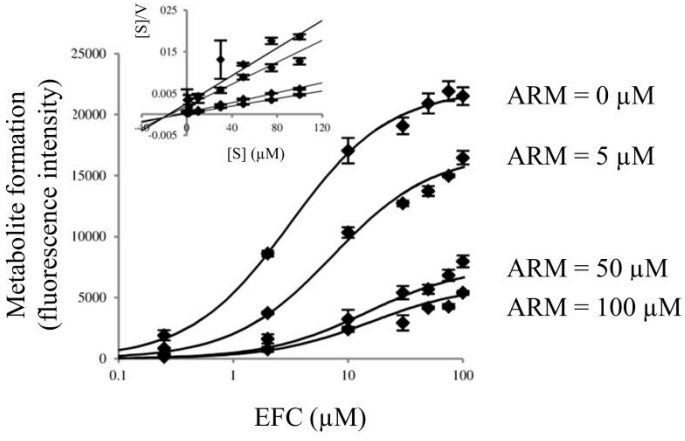

Figure 9. Observed (diamonds) and predicted (lines) formation of HFC, represented by the fluorescence intensity, from EFC (substrate, S) in rCYP2B6 in the absence and presence of varying concentrations of artemether (ARM). Predictions were obtained by simultaneously fitting a partial mixed inhibition model to the pooled data. Observed data in the graph are presented as mean ± SE (n = 4). Inset: Hanes-Woolf plot for the inhibition of HFC formation in rCYP2B6 by ARM.

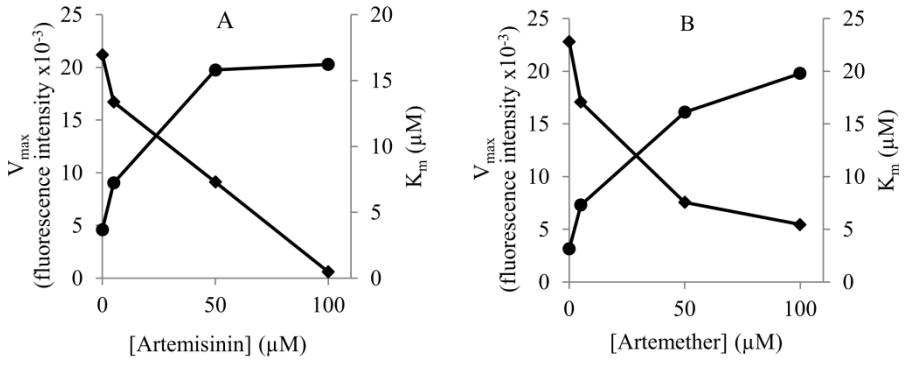

Figure 10. Kinetic parameters estimated by nonlinear regression (Michaelis-Menten equation) for the formation of HFC from EFC in rCYP2B6 in the absence and presence of increasing (A) artemisinin and (B) artemether concentrations.

4.1.2 Microsomal CYP2B6 activity

In microsomal incubations artemisinin and ARM inhibited the CYP2B6 activity by suppressing the formation of 8-hydroxyefavirenz from efavirenz, with estimated IC_{50} values of 9.07 ± 0.99 μM and 5.36 ± 0.52 μM, respectively. DHA did not show any inhibition on microsomal CYP2B6 activity.

4.1.3 Predicted change in drug exposure *in vivo*

The AUC ratios, calculated based on the estimated K_i values from the rCYP2B6 incubations, indicated a medium to high risk for DDI for artemisinin depending on what *in vivo* concentration used ($[I]_{max,u}$ or $[I]_{max,inlet,u}$). For ARM the risk for DDI was predicted to be low, with calculated AUC ratios below 1.1 regardless of what *in vivo* concentration used.

4.2 Paper II – CYP inhibition by artemisinin antimalarials *in vitro*

4.2.1 Recombinant CYP (rCYP) activity

IC_{50}, K_i and mechanism of inhibition

All artemisinin endoperoxides but ARS inhibited two or more recombinant CYP isoforms (Table 4). All rCYP inhibitions described, except the DHA mediated inhibition of rCYP2C19 activity, were characterized by decreasing apparent V_{max} values and increasing apparent K_m values with increasing concentrations of inhibitor, indicating mixed type of inhibition (Fig. 11). Increasing concentrations of DHA in the presence of rCYP2C19 did result in decreased apparent V_{max} but unchanged K_m, indicating a noncompetitive inhibition mechanism (Fig. 11). In accordance with these results, the inhibition of rCYP1A2 by artemisinin and DHA, as well as the inhibition of both rCYP2B6 and rCYP2C19 by artemisinin and ARM, were best described by a partial mixed inhibition model as defined by Equation 10 in section 4.1.1. A partial noncompetitive inhibition model, as defined by Equation 11, best described the DHA mediated inhibition on rCYP2C19.

$$V = \frac{V_{max}}{\left(1 + \frac{Km}{S}\right) \cdot \left(1 + \frac{I}{K_i}\right) \Big/ \left(1 + \frac{I \cdot \beta}{K_i}\right)} \qquad \text{(Eq. 11)}$$

where V represents the rate of metabolite formation, V_{max} the maximal rate of metabolite formation, S and I are the concentrations of substrate and inhibitor, respectively, and K_m is the Michaelis-Menten constant. As for the mixed type of inhibition, the decrease in V_{max} due to noncompetitive inhibition is described by the term β. Observed and predicted inhibition based on Equation 10 and 11 are shown in Fig. 12 for artemisinin, ARM and DHA on rCYP1A2, 2B6, and 2C19, respectively. Estimated parameter values are presented in Table 5.

4.2.2 Microsomal CYP activity

Analytical LC-MS/MS method

The adopted LC-MS/MS method previously described by Kim *et al.* [88] was optimized on an API 3000 triple quadropole mass spectrometer, and was sensitive enough to successfully quantify formed metabolites as

acetaminophen (CYP1A2), 7-hydroxycoumarin (CYP2A6), hydroxybupropion (CYP2B6), 4-hydroxytolbutamide (CYP2C9), dextrorphan (CYP2D6), and 1-hydroxymidazolam (CYP3A4). Further optimizing of the method on an API 4000 triple quadropole mass spectrometer was required for the quantification of very low concentrations of 4´-hydroxymephenytoin.

IC_{50} determination

In microsomal incubations all artemisinin endoperoxides inhibited at least one CYP isoform. Compared to the inhibition assay using recombinant enzymes, the IC_{50} values obtained in HLM were in the same order of magnitude (Table 4).

Table 4. IC_{50} values (µM) estimated by nonlinear regression for the inhibition of recombinant (rCYP) and microsomal (HLM) CYP1A2, 2B6, 2C19 and 3A4 activity by artemisinin, artemether, artesunate and dihydroartemisinin, respectively.

CYP isoform	ART	ARM	ARS	DHA
1A2: rCYP	6.3 ± 0.8[b]	NE	NE	13.1 ± 2.4[a]
HLM	1.4 ± 0.2[b]	NE	12.8 ± 1.2[b]	7.2 ± 1.1[b]
2B6: rCYP	7.4 ± 1.4[a]	2.4 ± 0.5[b]	NE	NE
HLM	12.8 ± 1.b[2]	2.9 ± 0.4[b]	NE	NE
2C19: rCYP	15.0 ± 4.5[a]	18.3 ± 2.3[a]	NE	21.9 ± 3.8[a]
HLM	10.9 ± 0.9[b]	9.2 ± 1.1[a]	NE	13.0 ± 1.3[b]
3A4: rCYP	NE	NE	NE	NE
HLM	18.1 ± 2.5[b]	34.4 ± 10.3[b]	NE	NE

Abbreviations: ART, artemisinin; ARM, artemether; ARS, artesunate; DHA, dihydroartemisinin; NE, not estimated

[a] Parameter estimate ± SE based on Equation 6 (gamma = 1) (n = 4); values in molar unit (µM)

[b] Parameter estimate ± SE based on Equation 6 (gamma estimated) (n = 4); values in molar unit (µM)

Table 5. Enzyme kinetic parameters (K_m, V_{max} and K_i) for artemisinin, artemether and dihydroartemisinin incubated with rCYP1A2, 2B6 and 2C19, respectively, estimated by nonlinear regression analysis. For partial mixed inhibition, the decrease in binding affinity (increased apparent K_m) is described by the term α (>1). The decrease in apparent V_{max} for both partial mixed inhibition and partial noncompetitive inhibition is defined by the term β. Data presented as parameter estimate ± SE (n=4).

CYP	Inhibitor	V_{max} [a]	K_m (μM)	K_i (μM)	α	β
1A2	ART[b]	28.7 ± 0.5	0.8 ± 0.05	1.0 ± 0.1	3.2 ± 0.6	0.17 ± 0.02
1A2	DHA[b]	33.7 ± 0.6	1.2 ± 0.07	3.4 ± 0.4	5.8 ± 1.2	0.29 ± 0.03
2B6	ART[b]	14.4 ± 0.3	4.3 ± 0.5	6.2 ± 1.5	3.7 ± 1.1	0.13 ± 0.04
2B6	ARM[b]	26.4 ± 0.5	5.6 ± 0.6	2.7 ± 0.5	17 ± 7.0	0.38 ± 0.08
2C19	ART[b]	22.5 ± 0.4	4.2 ± 0.4	1.4 ± 0.3	1.6 ± 0.2	0.58 ± 0.03
2C19	ARM[b]	28.9 ± 0.7	6.6 ± 0.7	9.1 ± 2.1	1.6 ± 0.4	0.18 ± 0.04
2C19	DHA[c]	32.3 ± 0.6	8.7 ± 0.5	48.9 ± 9.3	-	0.18 ± 0.06

[a] Maximal fluorescence intensity ($_{\times}10^{-3}$).

[b] Parameter estimates based on a partial mixed inhibition model (Equation 10).

[c] Parameter estimates based on a partial noncompetitive inhibition model (Equation 11).

4.2.3 Predicted change in drug exposure *in vivo*

The AUC ratios, calculated based on the estimated K_i values from the rCYP incubations, indicated a high risk of DDI *in vivo* for artemisinin if coadministrated with a CYP1A2 or 2C19 substrate, while a medium risk was predicted with a CYP2B6 substrate. For DHA on CYP1A2 the predicted risk based on $[I]_{max,inlet,u}$ was medium, but low if based on $[I]_{max,u}$. A low risk of DDI was also predicted for DHA on CYP2C19, and for ARM on CYP2B6 and 2C19, repectively.

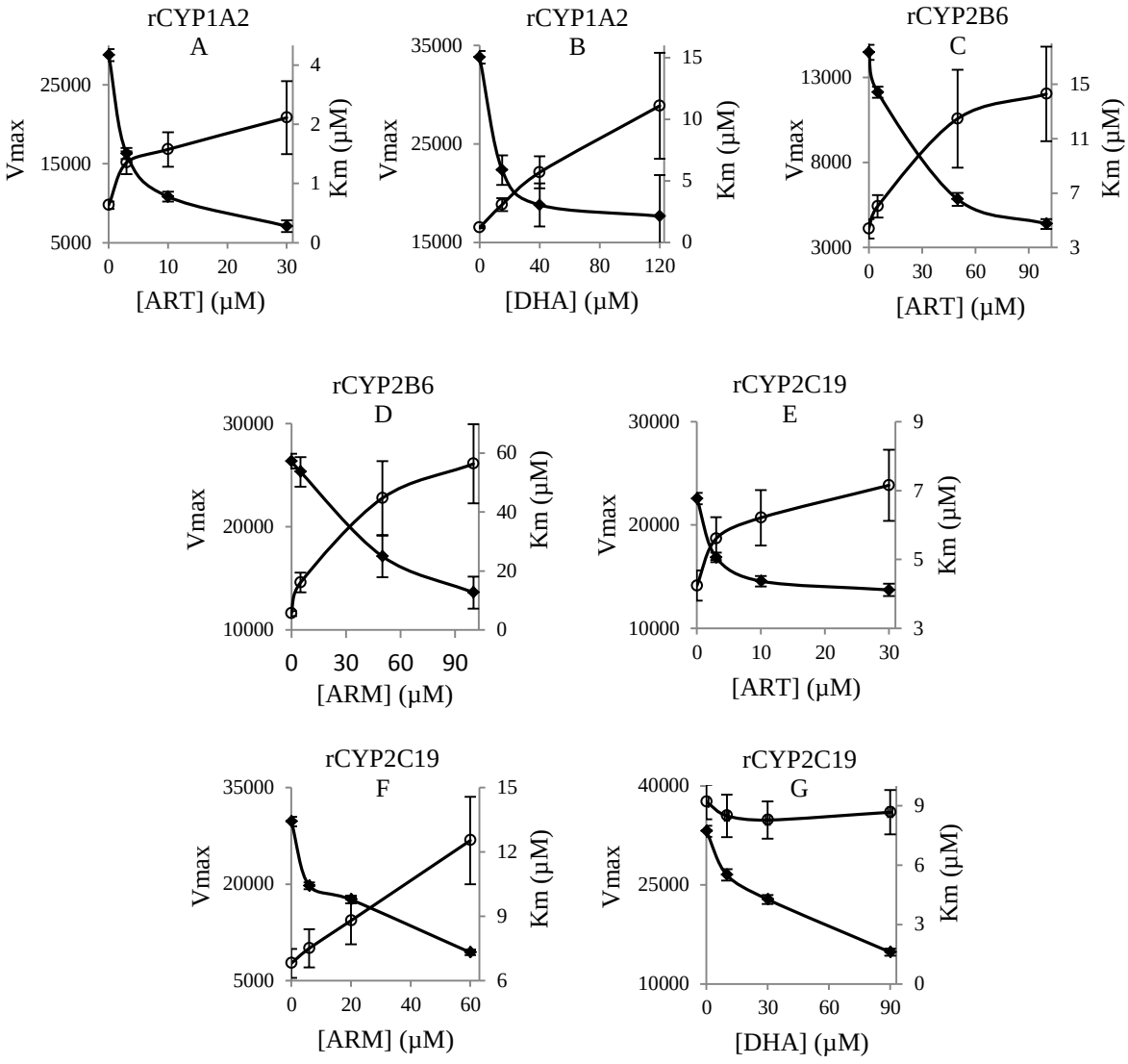

Figure 11. Apparent V_{max} values (closed diamonds) and apparent K_m values (open circles) for the formation of fluorescent metabolites (see Methods) in recombinant enzymes in the absence and presence of increasing concentrations of artemisinin (ART), artemether (ARM) and dihydroartemisinin (DHA). Apparent kinetic parameters are estimated by nonlinear regression (Michaelis-Menten equation), and data are presented as parameter estimates ± SE (n=4). Maximal metabolite formation rates (V_{max}) are represented by the fluorescence intensity. Inhibition of rCYP1A2 by ART (A) and DHA (B); inhibition of rCYP2B6 by ART (C) and ARM (D); inhibition of rCYP2C19 by ART (E), ARM (F) and DHA (G).

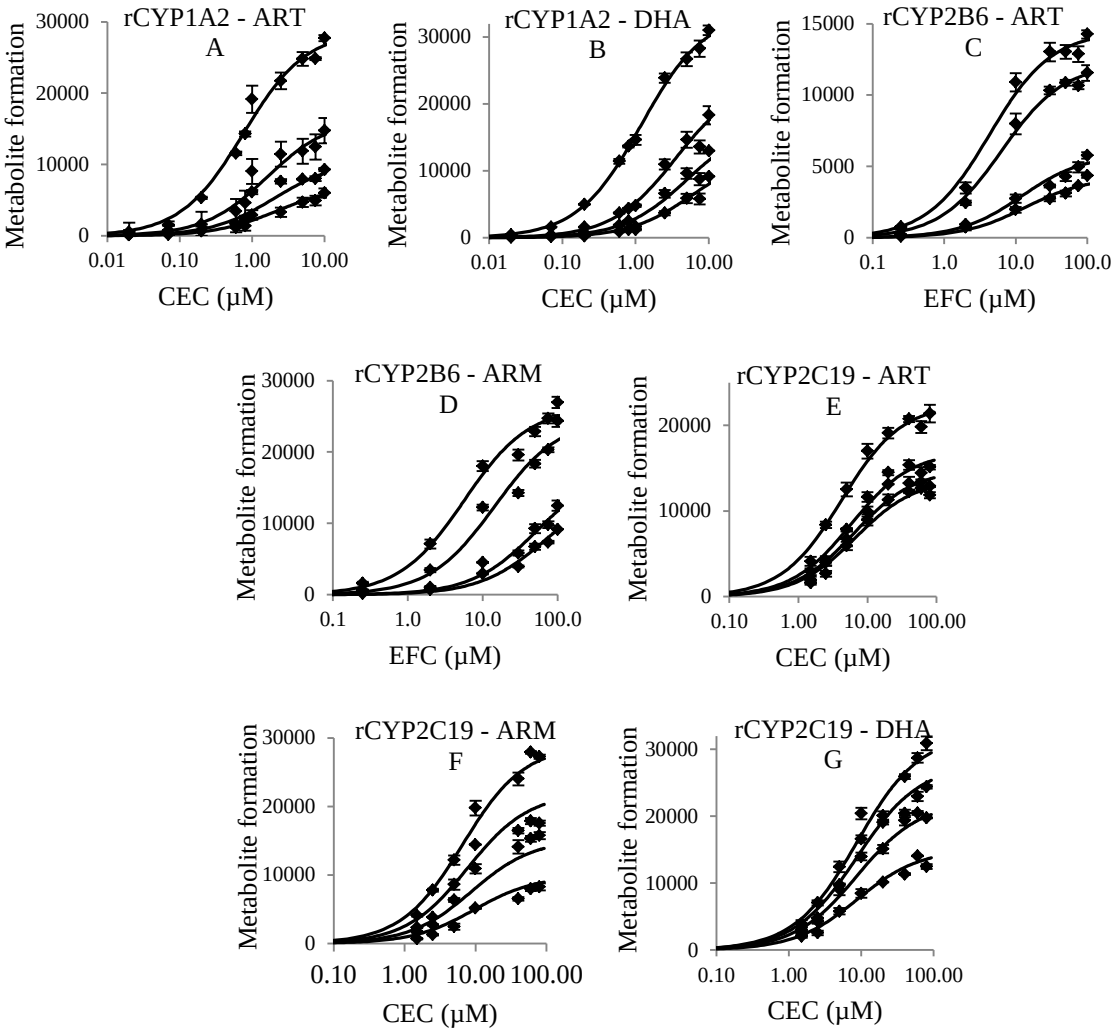

Figure 12. Observed (diamonds) and predicted (lines) formation of fluorescent metabolites (see Methods), represented by the fluorescence intensity, in recombinant enzymes in the absence and presence of increasing concentrations of artemisinin (ART), artemether (ARM) and dihydroartemisinin (DHA). The predicted inhibition of rCYP1A2 by ART (A) and DHA (B), of rCYP2B6 by ART (C) and ARM (D), and of rCYP2C19 by ART (E) and ARM (F), respectively, are all based on a partial mixed inhibition model (Equation 10) fitted to the pooled data. The predicted inhibition of rCYP2C19 by DHA (G) is based on a partial noncompetitive inhibition model (Equation 11). Observed data in the graphs is presented as mean ± SE (n=4).

4.3 Paper III – Bioanalytical method for quantification of ARS and DHA in human plasma and saliva

4.3.1 Sample preparation and LC–MS/MS assay

The choice of the SPE sorbent and the operating conditions are crucial for obtaining high degree of purification and good recoveries of the analytes of interest. After evaluation of several SPE products and experimental conditions, a HyperSep Retain PEP 96-well plate was used for the extraction of ARS, DHA and artemisinin as IS from plasma and saliva. The analytes were eluted using methanol-acetonitrile (90:10, v/v), resulting in high and reproducible recoveries for ARS (98-102%), DHA (91.2-104%), and IS (97.2-99.9%) in the two biological matrices.

The same chromatographic conditions, previously optimized for the analysis of ARS, DHA and IS in rat plasma, were successfully implemented for the analysis of human plasma and saliva samples.

4.3.2 Method validation

The method was fully validated in accordance with FDA guidelines [83].

Validation parameters:

- *Calibration range:* Quadratic regression and the peak area ratio of analyte/IS were used to generate the calibration curve, ranging from 5 to 1000 ng/mL for ARS (Supplement 1) and from 5 to 2000 ng/mL for DHA (Supplement 2).
- *Sensitivity:* LLOQ was set to 5 ng/mL for ARS and DHA in plasma and saliva, respectively, with deviation from the nominal concentrations being <20%.
- *Accuracy:* The intra-day and inter-day accuracy were high and within the acceptable limits to meet the guidelines for both ARS and DHA in plasma (Table 6) and saliva (Table 7).
- *Precision:* The intra-day and inter-day precision were high and within the acceptable limits to meet the guidelines for both ARS and DHA in plasma (Table 6) and saliva (Table 7).
- *Selectivity*: No interference between ARS, DHA and IS was seen and all analytes were well separated with sharp peaks at retention times 3.0, 2.3, and 4.0 min, respectively, in both plasma (Fig. 13) and saliva (Fig. 14). The absence of ion suppression was demonstrated by

post-column infusion experiments for all three analytes in plasma (Fig. 13) and saliva (Fig. 14), respectively.

- *Stability*: ARS, DHA and IS were demonstrated to be stable under the handling/processing conditions specified for the current method. Short-term temperature stability tests indicated degradation of ARS and DHA in plasma and saliva after 24 and 4 hours, respectively, at ambient temperature (Table 8). To preserve sample integrity and minimize analyte degradation, all handling of samples was performed on ice.

4.3.3 Application to clinical plasma and saliva samples

The LC-MS/MS assay was successfully applied on clinical plasma and saliva samples from patients with breast cancer receiving oral treatment with ARS. Data included in paper III is from a representative patient, receiving a single oral ARS dose (200 mg).

Table 6. Intra-day and inter-day accuracy and precision for artesunate (ARS) and dihydroartemisinin (DHA) in human plasma. Calculated concentrations (ng/mL) are presented as average ± SD and precision represented by the %CV.

[Nominal] (ng/mL)		**Intra-day (n=5)**			**Inter-day (n=15)**		
		[Calculated] (ng/mL)	**Accuracy**	**%CV**	**[Calculated] (ng/mL)**	**Accuracy**	**%CV**
ARS	5	4.98±0.05	99.6	0.9	4.97±0.21	99.5	4.2
DHA	5	5.03±0.07	101	1.4	5.05±0.12	101	2.5
ARS	15	14.6±0.45	97.4	3.1	14.6±1.08	97.4	7.4
DHA	15	15.0±0.26	100	1.7	15.1±0.30	100	2.0
ARS	300	307±6.87	102	2.2	298±12.3	99.2	4.1
DHA	750	787±35.5	105	4.5	763±37.2	101	4.9
ARS	750	763±17.3	102	2.3	737±35.1	98.3	4.8
DHA	1500	1506±60.2	100	4	1412±111	94.1	7.8

Table 7. Intra-day and inter-day accuracy and precision for artesunate (ARS) and dihydroartemisinin (DHA) in human saliva. Calculated concentrations (ng/mL) are presented as average ± SD and precision represented by the %CV.

[Nominal] (ng/mL)		Intra-day (n=5)			Inter-day (n=15)		
		[Calculated] (ng/mL)	Accuracy	%CV	[Calculated] (ng/mL)	Accuracy	%CV
ARS	5	4.99±0.06	99.8	1.3	4.97±0.09	99.5	1.9
DHA	5	5.01±0.07	100	1.3	5.0±0.07	100	1.4
ARS	15	15±0.10	100	0.7	15.0±0.15	100	1.0
DHA	15	15±0.11	100	0.7	15.0±0.17	99.9	1.1
ARS	300	301±5.30	100	1.8	301±4.67	100	1.6
DHA	750	751±13.6	100	1.8	747±16.5	99.6	2.2
ARS	750	759±9.10	101	1.2	741±23.2	98.8	3.1
DHA	1500	1518±26.8	101	1.8	1496±25.6	99.7	1.7

Table 8. Short-term stability of artesunate (ARS) and dihydroartemisinin (DHA) in plasma and saliva, respectively (n = 3). Data presented as % remaining analyte in stored samples compared to initial conditions (average ± SD).

Analyte nominal concentration (ng/mL)	Stability (%) in plasma	Stability (%) in saliva
Short-term temperature stability (4 hr at room temp.)		
ARS 75	96.5±3.73	83.9±3.35
ARS 750	100±10.9	86.1±0.20
DHA 100	96.8±5.34	91.8±0.88
DHA 1000	94.6±5.38	90.7±2.84
Short-term temperature stability (24 hr at room temp.)		
ARS 75	75.7±1.98	-
ARS 750	77.4±6.43	-
DHA 100	53.2±2.70	-
DHA 1000	42.9±2.63	-

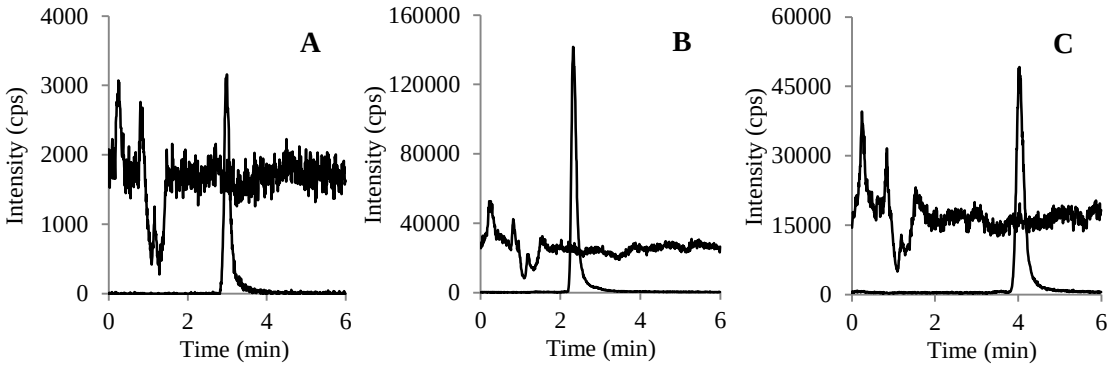

Figure 13. Injection of extracted blank human plasma during post-column infusion of (A) artesunate, (B) dihydroartemisinin, and (C) IS, with overlay of chromatograms representing calibration standards of respective analyte (ARS, DHA and IS at 500, 1000 and 1000 ng/mL, respectively).

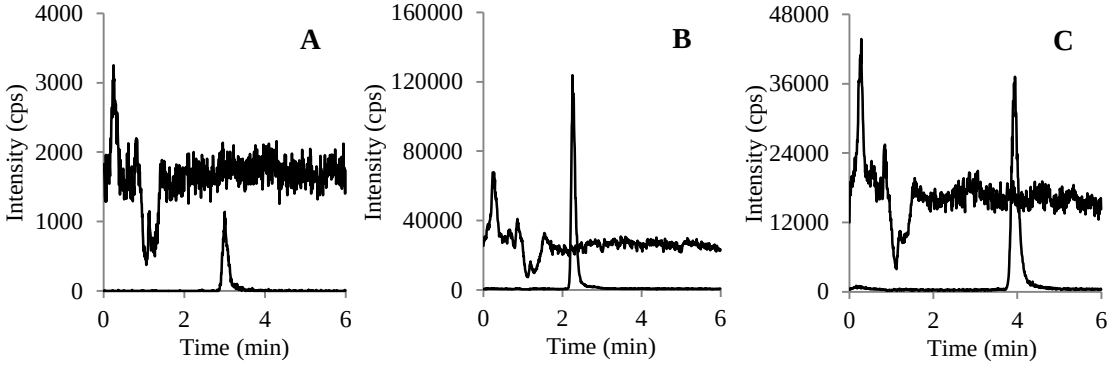

Figure 14. Injection of extracted blank human saliva during post-column infusion of (A) artesunate, (B) dihydroartemisinin, and (C) IS, with overlay of chromatograms representing calibration standards of respective analyte (ARS, DHA and IS at 500, 1000 and 1000 ng/mL, respectively).

4.4 Paper IV – Pharmacokinetics of ARS and DHA in patients with breast cancer

Altogether, data from six patients on 100 mg daily oral ARS doses, four patients on 150 mg, and seven patients on 200 mg, was included in the final pharmacokinetic analysis.

Both ARS and DHA were eliminated rapidly from the body with estimated elimination half-lives ($t_{1/2}$) of 0.95 (±0.75) and 1.81 (±0.42) hours after single dose, and 0.82 (±0.79) and 1.71 (±0.69) hours at steady state for ARS and DHA, respectively. As indicated by the large standard deviation, ARS revealed high variability in drug concentrations. No statistically significant changes between single dose and steady state C_{max}, T_{max} and AUC (all dose groups) were shown for ARS or DHA. Half-lives ($t_{1/2}$) remained unchanged, except in the 150 mg dose group where the $t_{1/2}$ for DHA was significantly reduced by 70% at steady state compared to after single dose. When analyzing all dose groups together, DHA clearance showed a statistically significant increase at steady state compared to after single dose. However, this increase did not reach statistical significance in the respective dose groups. Estimated pharmacokinetic parameters after single dose and at steady state for ARS and DHA are summarized in Table 9 and 10, respectively. Changes in plasma AUC for ARS and DHA after single dose compared to at steady state for each dose group are shown in Fig. 15.

Table 9. Pharmacokinetics of artesunate (ARS) after single-dose and long-term (>3 weeks) administration of oral ARS. Data presented as mean (± SD).

ARS 100 mg (n=6)	Single dose	Steady state	Paired t-test*
C_{max} (ng/mL)	51.6 (± 20.8)	89.9 (± 49.5)	0.20
T_{max} (h)	0.53 (± 0.38)	0.83 (± 0.55)	0.30
$AUC_{0-\infty}$ (ng/mL*h)	80.8 (± 25.6)	-	0.43
AUC_{0-24} (ng/mL*h)	-	79.8 (± 47.3)	
CL (L/h)	1472 (± 780)	2363 (± 2363)	0.43
$t_{1/2}$ (h)	1.41 (± 1.14)	0.68 (± 0.30)	0.24
ARS 150 mg (n=4)			
C_{max} (ng/mL)	87.2 (± 21.9)	127 (± 64.8)	0.17
T_{max} (h)	0.25 (± 0.01)	0.69 (± 0.37)	0.13
$AUC_{0-\infty}$ (ng/mL*h)	125 (± 36.5)	-	0.84
AUC_{0-24} (ng/mL*h)	-	126 (± 37.3)	
CL (L/h)	1294 (± 337)	1292 (± 349)	0.84
$t_{1/2}$ (h)	0.84 (± 0.15)	1.05 (± 0.37)	0.15
ARS 200 mg (n=7)			
C_{max} (ng/mL)	240 (± 264)	315 (± 228)	0.21
T_{max} (h)	0.80 (± 0.60)	0.58 (± 0.47)	0.50
$AUC_{0-\infty}$ (ng/mL*h)	190 (± 106)	-	0.28
AUC_{0-24} (ng/mL*h)	-	154 (± 80.2)	
CL (L/h)	1442 (± 990)	1954 (± 1571)	0.28
$t_{1/2}$ (h)	0.51 (± 0.25)	0.13 (± 0.12)	0.23
ARS all (n=17)			
CL (L/h)	1318 (± 729)	1977 (± 1698)	0.21

Table 10. Pharmacokinetics of dihydroartemisinin (DHA) after single dose and long-term (>3 weeks) administration of oral ARS. Data presented as mean (± SD).

ARS 100 mg (n=6)	Single dose	Steady state	Paired t-test*
C_{max} (ng/mL)	201 (± 62.8)	256 (± 67.4)	0.38
T_{max} (h)	1.38 (± 0.50)	1.91 (± 0.64)	0.28
$AUC_{0-\infty}$ (ng/mL*h)	511 (± 94.5)	-	0.95
AUC_{0-24} (ng/mL*h)	-	510 (± 69.3)	
CL (L/h)	150 (± 29.9)	148 (± 20.5)	0.95
$t_{1/2}$ (h)	1.79 (± 0.41)	1.70 (± 0.80)	0.73
ARS 150 mg (n=4)			
C_{max} (ng/mL)	337.5 (± 47.9)	328 (± 107)	0.63
T_{max} (h)	1.65 (± 0.85)	1.51 (± 0.53)	0.87
$AUC_{0-\infty}$ (ng/mL*h)	909 (± 219)	-	0.18
AUC_{0-24} (ng/mL*h)	-	788 (± 220)	
CL (L/h)	131 (± 37.7)	151 (± 36.9)	0.18
$t_{1/2}$ (h)	1.90 (± 0.34)	1.34 (± 0.34)	0.03*
ARS 200 mg (n=7)			
C_{max} (ng/mL)	787 (± 424)	714 (± 274)	0.68
T_{max} (h)	1.44 (± 0.81)	1.01 (± 0.40)	0.13
$AUC_{0-\infty}$ (ng/mL*h)	1629 (± 472)	-	0.06
AUC_{0-24} (ng/mL*h)	-	1070 (± 307)	
CL (L/h)	98.0 (± 25.8)	152 (± 49.7)	0.06
$t_{1/2}$ (h)	1.72 (± 0.44)	1.70 (± 0.80)	0.96
ARS All (n=17)			
CL (L/h)	124 (± 38.2)	150 (± 38.6)	*0.0440**

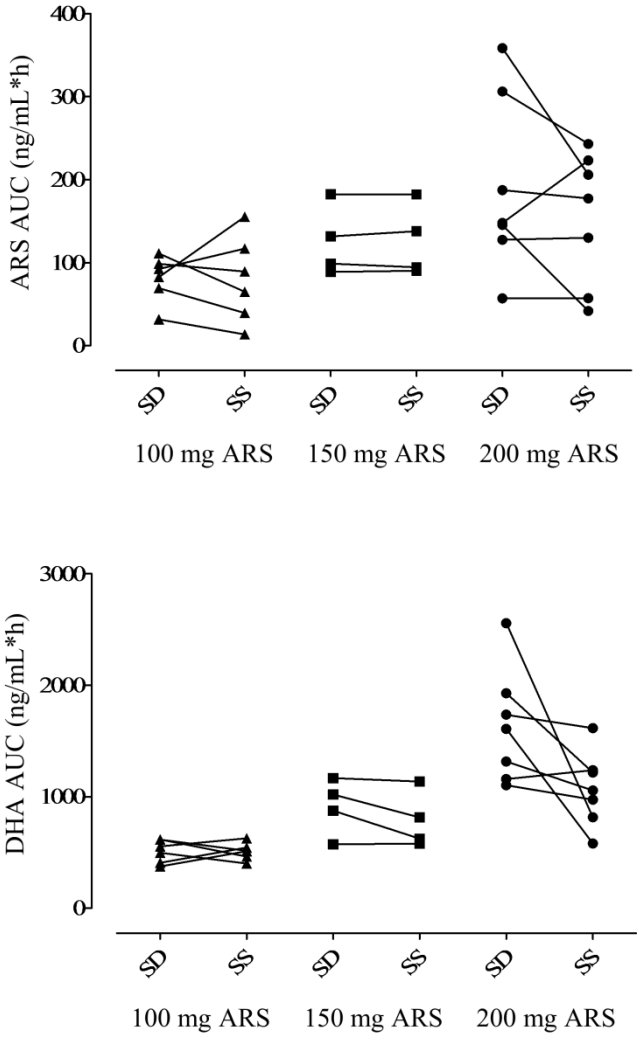

Figure 15. Individual changes in plasma AUC from single dose (SD) to steady state (SS) of artesunate (ARS; upper) and dihydroartemisinin (DHA; lower), respectively, after intake of 100 mg (circles), 150 mg (squares), or 200 mg (triangle) oral ARS.

4.5 Paper V – Population pharmacokinetics of ARS and DHA in patients with breast cancer

A total of 640 ARS and DHA plasma concentrations, respectively, and 614 DHA saliva concentrations from twenty-three patients were included in the population pharmacokinetic analysis. 41% and 20% of plasma ARS and DHA samples respectively, and 39% of DHA saliva samples were below the quantification limit (BQL). To handle BQL data, the M1, M3 and M6 methods (described in section 3.4.2) were evaluated. Considering the relatively large amount of BQL data, and based on GOF plots, the M6 method was implemented, including only the first BQL sample in a consecutive seried (imputed as LLOQ/2) while excluding all other values below LLOQ.

A combined drug-metabolite model with a two-compartment disposition model for ARS and a one-compartment disposition model for DHA best described the pharmacokinetics of ARS and DHA in plasma (Fig. 16) when including full drug concentration-profile data and sparse sample data. The inclusion of a peripheral compartment for ARS resulted in a significant drop in OFV (ΔOFV = -438). ARS absorption from the dosing compartment to the central compartment was adequately described by a first-order absorption process without lag time. Inclusion of a relative bioavailability, with a population value fixed to 100% and BSV estimated, improved the model fit (ΔOFV = -62.6). Models describing enterohepatic recirculation or partial pre-systemic conversion of ARS to DHA resulted in no decrease in OFV and were omitted from the final model. Allometric scaling with BW on apparent clearance parameters and apparent volumes of distribution did not improve the model fit (ΔOFV = 3.7) and were not included. No other evaluated covariates could explain the BSV that was estimated for $V_{C,ARS}/F$, k_a, relative bioavailability and CL_{DHA}/F. An estimated slope factor of 0.116 described the relationship between salivary DHA and plasma DHA.

From here on, the final structural model when including full plasma and saliva concentration-time profile data and sparse sample data will be referred to as model A. The model described the observed plasma and saliva data adequately (GOF plots presented as Supplement 1). Population parameter estimates and BSV estimates for model A are summarized in Table 11. Predicted-corrected VPC plots showing a good predictive performance of the model are shown in Fig. 17.

A time-dependent increase (24.9%) in elimination clearance of DHA (CL_{DHA}/F) was observed when analyzing full drug concentration-time profile data after the first oral ARS dose and after at least three weeks daily medication (model B). The model described the observed plasma data adequately (GOF plots presented as Supplement 2). Good predictive performance of the model is demonstrated by the predicted-corrected VPC plots (Fig. 17). Population parameter estimates and BSV estimates are summarized in Table 12.

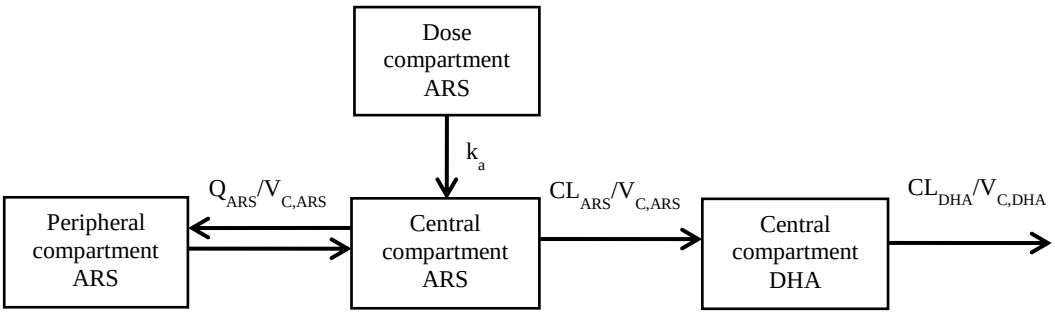

Figure 16. Structural model for artesunate (ARS) and dihydroartemisinin (DHA) plasma pharmacokinetics in patients with breast cancer after oral administration of ARS. k_a, first-order absorption rate constant; V_C, apparent volume of distribution of the central compartment; V_P, apparent volume of distribution of the peripheral compartment; CL, oral/apparent elimination clearance; Q, apparent intercompartmental clearance.

Table 11. Parameter estimates describing the population pharmacokinetics of artesunate (ARS) and dihydroartemisinin (DHA) in plasma, and the relationship between salivary and plasma DHA (model A).

	Population estimates[a] [% RSE][b]	**95% CI[b]**	**BSV[a] [% RSE][b]**	**95% CI for BSV[b]**
Artesunate plasma				
CL_{ARS}/F (L/h)	1260 [11.1]	1249;1271	-	-
$V_{C,ARS}/F$ (L)	1160 [16.6]	1145;1175	52.4 [31.1]	45.2;59.6
Q_{ARS}/F (L/h)	258 [16.6]	255;261	-	-
$V_{P,ARS}/F$ (L)	1320 [23.7]	1295;1345	-	-
k_a (h^{-1})	3.35 [33.9]	3.26;3.44	160 [37.9]	141;179
$\sigma_{ARS,plasma}$	0.762 [6.01]	0.758;0.766	-	-
Bioavailability	1 FIX	-	41.9 [33.5]	35.6;48.2
Dihydroartemisinin plasma				
CL_{DHA}/F (L/h)	118 [8.23]	117;119	23.1 [50.6]	18.7;27.5
$V_{C,DHA}/F$ (L)	98.0 [12.8]	97.0;99.0	-	-
$\sigma_{DHA,plasma}$	0.558 [5.08]	0.556;0.560	-	-
Dihydroartemisinin saliva				
Θ_1	0.116 [5.04]	0.115;0.116	-	-
$\sigma_{DHA,saliva}$	0.654 [4.71]	0.652;0.656	-	-

CL_{ARS}/F: elimination clearance of ARS, $V_{C,ARS}/F$: apparent volume of distribution of the central compartment of ARS, Q_{ARS}/F: intercompartmental clearance of ARS between the central and the peripheral compartment, $V_{P,ARS}/F$: apparent volume of distribution of the peripheral compartment for ARS, CL_{DHA}/F: elimination clearance of DHA, V_{DHA}/F; apparent volume of distribution of DHA, F; relative bioavailability, k_a; first-order absorption rate constant. The additive error (σ) variance will essentially be exponential on arithmetic scale data. Coefficient of variation (%CV) for BSV was calculated as $100*((e^{\text{mean variance estimate}})-1)^{1/2}$. Relative standard error (RSE) was calculated as 100*(standard deviation/mean value). The 95% confidence intervals (CI) are given as the 2.5 to 97.5 percentiles of bootstrap estimates.

[a] Based on population mean values from NONMEM

[b] % RSE and 95% CI for parameters are based on 683 successful stratified bootstrap runs (out of 750 runs)

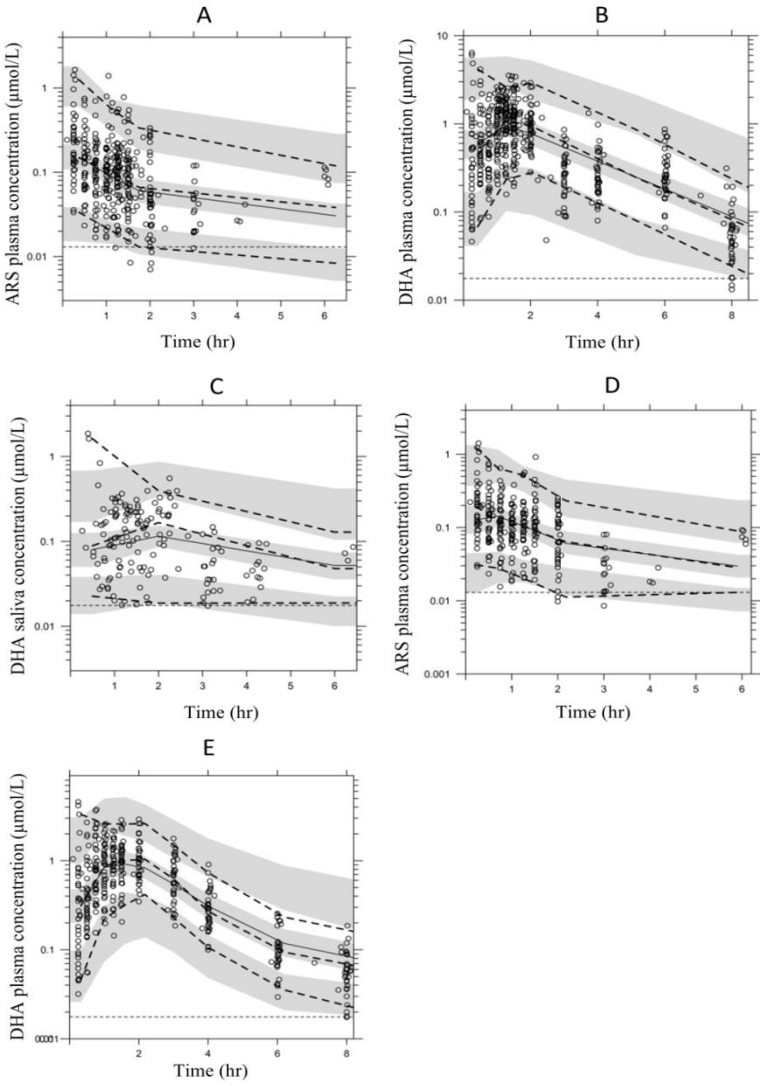

Figure 17. Predicted-corrected visual predictive check of the final models; model A for artesunate (ARS) in plasma (A), dihydroartemisinin (DHA) in plasma (B), and DHA in saliva (C), and model B for ARS in plasma (D), and DHA in plasma (E), respectively. Observations and the 5th, 50th and 95th percentile of observed data are presented as circles and dashed lines, respectively. Solid lines represent the 50th percentile of simulated plasma concentrations of ARS and DHA, respectively. Shaded areas represent the simulated 95% confidence interval of the 5th, 50th and 95th percentiles of simulated plasma concentrations. Dashed horizontal lines represent LLOQ for ARS (0.013 µM) and DHA (0.018 µM), respectively. Time is presented as time after dose, and is restricted to 6.5 hours for plasma ARS and salivary DHA, and to 8.5 hours for plasma DHA, respectively, excluding one observed DHA plasma concentration at 10.4 h when sparse samples were included (plot B).

Table 12. Parameter estimates describing the population pharmacokinetics of artesunate (ARS) and dihydroartemisinin (DHA) in plasma based on full concentration-time profile data from occasion 1 and 2 (model B).

	Population estimates[a] [% RSE][b]	**95% CI[b]**	**BSV[a] [% RSE][b]**	**95% CI for BSV[b]**
Artesunate plasma[a]				
CL_{ARS}/F (L/h)	1100 [15.4]	1088;1112	17.7 [62.5]	13.7;21.7
$V_{C,ARS}/F$ (L)	1280 [19.6]	1262;1298	48.8 [52.1]	39.5;58.1
Q_{ARS}/F (L/h)	213 [55.8]	202;224	-	-
$V_{P,ARS}/F$ (L)	930 [203]	485;1402	-	-
k_a (h^{-1})	2.88 [32.1	2.81;2.95	136 [40.0]	119;153
$\sigma_{ARS,plasma}$	0.695 [6.55]	0.692;0.698	-	-
Bioavailability	1 FIX	-	32.6 [30.9]	28.0;37.2
Dihydroartemisinin plasma[a]				
CL_{DHA}/F (L/h)	109 [15.3]	108;110	-	-
$V_{C,DHA}/F$ (L)	99.6 [18.2]	98.4;101	-	-
Θ_1	0.249 [29.6]	0.243;0.255	-	-
$\sigma_{DHA,plasma}$	0.549 [9.58]	0.545;0.553	-	-

CL_{ARS}/F: elimination clearance of ARS, $V_{C,ARS}/F$: apparent volume of distribution of the central compartment of ARS, Q_{ARS}/F: intercompartmental clearance of ARS between the central and the peripheral compartment, $V_{P,ARS}/F$: apparent volume of distribution of the peripheral compartment for ARS, CL_{DHA}/F: elimination clearance of DHA, V_{DHA}/F; apparent volume of distribution of DHA, F; relative bioavailability, k_a; first-order absorption rate constant, Θ_1; relative change in CL_{DHA}/F between occasion 1 and 2. The additive error (σ) variance will essentially be exponential on arithmetic scale data. Coefficient of variation (%CV) for BSV was calculated as $100*((e^{\text{mean variance estimate}})-1)^{1/2}$. Relative standard error (RSE) was calculated as 100*(standard deviation/mean value). The 95% confidence intervals (CI) are given as the 2.5 to 97.5 percentiles of bootstrap estimates.

[a] Based on population mean values from NONMEM

[b] % RSE and 95% CI for plasma parameters are based on 746 successful stratified bootstrap runs (out of 1000 runs)

5 DISCUSSION

Artemisinin endoperoxides are being widely used in combination therapies in the treatment of malaria, but also have potential use in oncologic indications. This thesis has demonstrated the inhibitory effects on several drug metabolizing CYP enzymes exerted by the artemisinin endoperoxides (**Papers I** and **II**). Concomitant administration with drugs metabolized by CYP isoforms that are subject to artemisinin-induced inhibition could result in unwanted effects, such as toxicity or, in the case of prodrugs, insufficient therapeutic effect. This may be an issue in the treatment of patients that are co-infected with malaria and human immunodeficiency virus infection/acquired immunodeficiency syndrome (HIV/AIDS). Like malaria, HIV/AIDS is a widely spread disease in African countries. Considering the geographical overlap between the two diseases, and the fact that HIV-infected patients are at increased risk of suffering from malaria infection, a substantial number of co-infections occurs. Concomitant treatment with malaria therapy (ACT) and antiretroviral medicines for the HIV-infection increases the risk of unwanted drug interactions. The concern with inhibitory and inductive effects of artemisinin compounds is greater if artemisinin endoperoxides are to be used in cancer therapy. Based on IVIVE using *in vivo* concentrations observed after doses used in malaria treatment, data presented in this thesis indicates a potential risk of DDI *in vivo* for these compounds if coadministrated with drugs that are subject to metabolism by certain CYP enzymes (CYP1A2, 2B6 and 2C19). Oncologic indications would most likely require higher therapeutic concentrations of artemisinin endoperoxides than those used for the treatment of malaria [6, 93], and with long-term use the likely mode of therapy. This further increases the risk of clinically relevant drug interactions. If used as add-on therapy in cancer, concomitant administration with other drugs is inevitable. One example being the estrogen receptor (ER) antagonist tamoxifen, which is the standard endocrine therapy for hormone receptor-positive breast cancer, and is often given to patients with early stages of breast cancer or with metastatic breast cancer [94]. Tamoxifen acts as a prodrug, being bioactivated by the Cytochrome P450 enzyme system to active metabolites, which exert higher binding affinity to the ER receptor and enhanced potency compared to the parent compound. CYP2B6 and 2C19 have been demonstrated to contribute to the bioactivation of tamoxifen *in vitro* [95], two CYP isoforms that, in this thesis, have been shown to be inhibited by artemisinin endoperoxides. This might be a concern if artemisinin endoperoxides are to be given together with tamoxifen in breast cancer treatment, since it could result in reduced bioactivation of tamoxifen and insufficient therapeutic effect.

The pharmacokinetics of artemisinin and its derivatives have been extensively investigated and reported in literature. However, existing data is based on observations in healthy volunteers or malaria patients after single dose or short-term (≤7 days) regimens. This thesis contributes with novel pharmacokinetic characteristics of ARS and its active metabolite DHA after long-term (>3 weeks) treatment with orally administrated ARS once daily to patients with metastatic breast cancer. A combined drug-metabolite model, with first-order absorption of ARS from the dose compartment followed by a two-compartment disposition model for ARS and a one-compartment disposition model for DHA, best described the observed data. Population parameter estimates of CL/F and V/F for ARS and DHA presented in this thesis (**Paper V**) were in good agreement with values for healthy volunteers reported in literature [34]. Values of CL/F for both compounds estimated based on population pharmacokinetic modelling or non-compartmental analysis (**Paper IV**), respectively, were similar. Both analyses indicated an increase in apparent elimination clearance of DHA after three weeks of daily oral ARS medication. Time-dependent pharmacokinetics has previously been demonstrated for artemisinin endoperoxides [64-66], an effect that has been attributed to autoinduction of CYP enzymes [67]. DHA is generally considered to be metabolized by glucuronidation, a reaction mainly catalyzed by UGT1A9 and UGT2B7 [96]. Although not reported for ARS or DHA, inductive effects on UGT enzymes in human subjects have been demonstrated [97-98]. Autoinduction of any of the UGTs involved in the glucuronidation of DHA cannot be excluded as the underlying mechanism for the time-dependent increase in CL_{DHA}/F observed in patients with breast cancer. However, although glucuronidation is generally considered the primary route of DHA elimination, it should not be ruled out that oxidative processes by the Cytochrome P450 enzyme system may contribute. *In vitro* and *in vivo* studies have shown evidence of extensive phase I metabolism of DHA by CYP enzymes in rat liver microsomes [99], and identified hydroxylated and deoxyl phase I metabolites in rat bile, urine and plasma [100]. This might occur also in human being, and autoinduction of any CYP enzyme that may be involved in the metabolism of DHA could be the potential mechanism behind the time-dependent increase in CL_{DHA}/F reported here.

This thesis presents a bioanalytical method for the quantification of ARS and DHA in human saliva (**Paper III**). Quantification of ARS and DHA in saliva offers the possibility to use saliva sampling as a substitute for blood in therapeutic drug monitoring and pharmacokinetic investigations. Compared to blood sampling, saliva offers several advantages, including a noninvasive and inexpensive sampling technique that is manageable for untrained staff

and even for patients themselves. In general, more sensitive bioanalytical methods are required to detect drug concentrations in saliva, which usually are lower than those measured in plasma and, if distribution is rapid and pH-independent, roughly correspond to the unbound drug levels in blood [73, 75]. The multifactorial passage of drugs from the blood circulation to saliva can have extensive impact on the saliva/plasma concentration ratio, and for some drugs the salivary concentrations do not reflect the unbound levels in plasma. For artemisinin, Ashton *et al*. reported comparable salivary concentrations with the unbound artemisinin levels in plasma [81]. The distribution of ARS and DHA into saliva, two compounds with very different physicochemical properties, has not previously been reported in literature. With a relatively high lipophilicity and a high pK_a of 12.1 [101], DHA could easily passes through biological membranes in salivary glands. The high pK_a value makes DHA to be almost totally unionized in plasma and saliva [73], in contrast to the more hydrophilic ARS, which has a pK_a of 4.6 [102], making it >99% ionized in plasma (pH 7.4), and not prone for passive diffusion. Therefore, the concentration of DHA in saliva is more expected to reflect the unbound level in plasma, compared to ARS. This thesis demonstrates a correlation between salivary and plasma DHA, with an estimated proportionality constant of 0.116, which was in good agreement with previously reported values of unbound fraction of DHA in plasma [103]. This suggests a possible use of saliva sampling for therapeutic drug monitoring of DHA. Due to the fact that drug concentrations in saliva usually reflect unbound drug in plasma, salivary DHA may be more reflective of drug concentrations at the site of action than total DHA concentrations in plasma are.

.

6 CONCLUSION

One of the general conclusions in the present thesis is that artemisinin endoperoxides exert inhibitory effects on drug metabolizing CYP enzymes *in vitro*, but also show indications for autoinduction *in vivo*. Both effects could result in unwanted drug interactions if artemisinin class of compounds is to be given concomitantly with drugs that are eliminated by enzymes affected by the artemisinins. This may be an issue to consider in current treatment of patients that are co-infected with malaria and HIV/AIDS, as well as if the artemisinin endoperoxides are to be given in cancer therapy. Population analysis approach offers a useful tool to be able to separate between the effects of inhibition and induction on drug concentrations. By taking into account how different drugs interact, individual dosages can be optimized.

Specific conclusions from the studies included in this thesis were:

- Artemisinin, ARM, ARS and DHA were all shown to inhibit the activity of one or more CYP isoforms *in vitro*, including CYP1A2, 2B6, 2C19 and 3A4, which together account for the clearance mechanism for 60% of the drugs currently on the market. (**Papers I** and **II**)

- An LC-MS/MS assay for the quantification of ARS and DHA in human plasma and, for the first time in literature, in human saliva has been developed and validated according to regulatory guidelines. This offers the potential use of saliva sampling as an alternative to blood sampling in clinical trials including these two compounds. (**Paper III**)

- Despite a significant increase in oral clearance of DHA after long-term (<3 weeks) administration of oral ARS in patients with breast cancer, the pharmacokinetics of ARS and DHA were relatively stable and within bioequivalent margins, rendering ARS a good candidate for continued evaluation for oncologic indications. (**Paper IV**)

- Population pharmacokinetics of ARS and DHA after long-term use of oral ARS in patients with breast cancer were characterized and in good agreement with previously reported data. As indicated in paper IV, an almost 25% increase in elimination clearance of DHA was estimated,

which may be explained by autoinduction. Also, an estimated proportionality between salivary and plasma DHA concentrations was in good agreement with previously reported values of unbound fraction of DHA in plasma, and support the use of saliva sampling for therapeutic drug monitoring of DHA. (**Paper V**)

7 FUTURE PERSPECTIVES

During the past decades the artemisinin class of compounds has become the established treatment of *falciparum* malaria globally, and just until recently, they have been proven effective even against otherwise multidrug-resistant *P. falciparum*. However, alarming reports indicate resistance development toward artemisinin endoperoxides among malaria parasites [104-105]. Hopefully this will not mean the end of the successful era of artemisinin endoperoxides as antimalarial agents, but new hope may also be on their potential future use in the treatment of cancers. This thesis has contributed to a step closer the use of ARS/DHA as add-on therapy in patients with breast cancer, and further efficacy evaluation studies are motivated. If oncologic indications will be the future of these drugs, it is important to collect long-term data to be able to evaluate and estimate how the concentration changes with time, which of course may influence the effect over time.

This thesis has also opened up the possibilities for the future use of saliva as sampling matrix in clinical studies with ARS and DHA. Considering the ease and the inexpensiveness, saliva sampling would be favorable in resource limited settings. However, more studies are warranted to evaluate the robustness of the use of saliva measurements in order to predict the unbound DHA concentrations in plasma.

ACKNOWLEDGEMENT

I would like to give my deepest gratitude to all wonderful people that, in one way or another, made this thesis possible.

To my main supervisor **Michel Ashton**, for giving me the opportunity of doing my PhD study in the PKDM group, for allowing me to explore and develop my personal drive and scientific creativity, and for being a great source of knowledge.

To my co-supervisor **Angela Äbelö**, for always being supportive and encouraging when it comes to work and personal matters, for your great supervision and advising about many things, and for being a great source of wisdom and inspiration.

Kurt-Jürgen Hoffmann for valuable mentoring during the laboratory work, for your dedicated interest to help out and to share your great expertise within the field, and for many fruitful and encouraging discussions.

My co-authors: **Cornelia von Hagens** and **Antje Blank** with colleagues at the University Hospital in Heidelberg, for a constructive and good collaboration and your valuable contribution to my work, and for kindly welcoming me to visit in Heidelberg.

Many thanks to my fellow PhD students and co-workers in the PKDM group. **Sofia Birgersson**, for all your help and guidance during the LC-MS/MS work, for a great collaboration with our shared paper, and for being a great travel companion during long and delayed flights. **Richard Höglund**, for always being helpful and supportive when it comes to data modelling issues, and for being a great travel companion and photographer in Niagara Falls. **Elin Karlsson**, for contributing with great knowledge within bioanalysis and drug metabolism, and for your supportive and encouraging discussions. **Emile Bienvenu**, for your help and guidance during the HPLC work, and for being a great source of wisdom to the PKDM group. **Dinko Rekić**, for kindly introducing me to the NONMEM software. To all of you, including the past and presents colleagues **Carl Johansson**, **Karin Saalman** and **Mohd Yusmaidie**, thanks for sharing everyday life at the lab, and for contributing to a memorable time with fruitful discussions about work and other things in life.

To my master thesis students, **Angelica Torkelsson** and **Jesper Sundell**, for your dedicated work and valuable contribution to paper II. It was a pleasure to work with you and I wish you all the best.

To all colleagues at the Department of Pharmacology, with special thanks to: **Gunnar Tobin**, who first introduced me to the Department of Pharmacology when accepting me as a summer research student in his group during my pharmacy studies, and to **Michael Winder** and **Patrik Aronsson**, for being great co-workers during these two summers, **Annalena Carlred**, **Britt-Marie Benbow** and **Maria Björkevik** who in many ways have helped out with administrative issues, and **Agneta Ekman** and **Elisabet Jerlhag Holm**, who kindly accepted my request of being the chairman and a member of the grading committee, respectively, at my half-time seminar.

Kjell Stubberud at AB Sciexe, for all your kindly and most valuable help with bioanalytical instrumentation. Your help is invaluable to the PKDM group.

Ulrik Jurva at AstraZeneca for giving of your time and sharing of your great knowledge within mass spectrometry, and for your valuable contribution as a member of the grading committee at my half-time seminar.

Collen Masimirembwa for collaboration and input during the work of paper I.

Anna-Pia Palmgren at AztraZeneca for contributing with valuable input during the design of the time-dependent inhibition assay in paper I.

To all my beloved friends who in one way or another have inspired, supported and encouraged me, not only during my PhD studies, but also in life as a whole. I wish I could mention each and every one of you by name, but in lack of space I hope you know who you are. Your friendship means everything to me!

My dear friend **Anna Lundin**, thanks for all your inspiration and pep-talks during our numerous lunches at the "Medicinareberget", and for being a true friend.

Sara Karlsson for being a great friend and fellow PhD student, and for all your pep-talk and discussions about life, I believe in you!

To my beloved whole family, for always believing in me, your never ending support and your love. I can never say it to many times, I love each and every one of you! This thesis is for you.

Henrik, for being my inspiration in life and the flame of hope and love, I look forward to meet the future with you!

REFERENCES

[1] Rowland, M., Tozer, T. N., *Clinical pharmacokinetics and pharmacodynamics: concepts and applications*. **2011**

[2] Barrett, J. S., Fossler, M. J., Cadieu, K. D., Gastonguay, M. R., Pharmacometrics: a multidisciplinary field to facilitate critical thinking in drug development and translational research settings. *Journal of clinical pharmacology* **2008,** *48* (5), 632-49.

[3] Mould, D. R., Upton, R. N., Basic concepts in population modeling, simulation, and model-based drug development. *CPT: pharmacometrics & systems pharmacology* **2012,** *1*, e6.

[4] Mould, D. R., Upton, R. N., Basic concepts in population modeling, simulation, and model-based drug development-part 2: introduction to pharmacokinetic modeling methods. *CPT: pharmacometrics & systems pharmacology* **2013,** *2*, e38.

[5] *Guidelines for the treatment of malaria, 2nd edition*. World Health Organization (WHO), **2010**

[6] Efferth, T., Willmar Schwabe Award 2006: antiplasmodial and antitumor activity of artemisinin--from bench to bedside. *Planta medica* **2007,** *73* (4), 299-309.

[7] Firestone, G. L., Sundar, S. N., Anticancer activities of artemisinin and its bioactive derivatives. *Expert reviews in molecular medicine* **2009,** *11*, e32.

[8] Navaratnam, V., Mansor, S. M., Sit, N. W., Grace, J., Li, Q., Olliaro, P., Pharmacokinetics of artemisinin-type compounds. *Clinical pharmacokinetics* **2000,** *39* (4), 255-70.

[9] Bégué, J.-P., Bonnet-Delpon, D., The future of antimalarials: artemisinin and synthetic endoperoxides. *Drugs of the Future* **2005,** *30* (5), 509-518.

[10] Klayman, D. L., Qinghaosu (artemisinin): an antimalarial drug from China. *Science* **1985,** *228* (4703), 1049-55.

[11] Nosten, F., White, N. J., Artemisinin-based combination treatment of falciparum malaria. *The American journal of tropical medicine and hygiene* **2007,** *77* (6 Suppl), 181-92.

[12] Titulaer, H. A. C., Zuidema, J., Lugt, C. B., Formulation and pharmacokinetics of artemisinin and its derivatives. *Int J Pharm* **1991,** *69*, 83-92.

[13] Suputtamongkol, Y., Newton, P. N., Angus, B., Teja-Isavadharm, P., Keeratithakul, D., Rasameesoraj, M., Pukrittayakamee, S., White, N. J., A comparison of oral artesunate and artemether antimalarial bioactivities in acute falciparum malaria. *British journal of clinical pharmacology* **2001,** *52* (6), 655-61.

[14] Golenser, J., Waknine, J. H., Krugliak, M., Hunt, N. H., Grau, G. E., Current perspectives on the mechanism of action of artemisinins. *International journal for parasitology* **2006,** *36* (14), 1427-41.

[15] Vangapandu, S., Jain, M., Kaur, K., Patil, P., Patel, S. R., Jain, R., Recent advances in antimalarial drug development. *Medicinal research reviews* **2007,** *27* (1), 65-107.

[16] Vo, A. T., Millis, R. M., Epigenetics and breast cancers. *Obstetrics and gynecology international* **2012,** *2012*, 602720.
[17] White, N. J., Antimalarial drug resistance. *The Journal of clinical investigation* **2004,** *113* (8), 1084-92.
[18] Ndiaye, J. L., Randrianarivelojosia, M., Sagara, I., Brasseur, P., Ndiaye, I., Faye, B., Randrianasolo, L., Ratsimbasoa, A., Forlemu, D., Moor, V. A., Traore, A., Dicko, Y., Dara, N., Lameyre, V., Diallo, M., Djimde, A., Same-Ekobo, A., Gaye, O., Randomized, multicentre assessment of the efficacy and safety of ASAQ--a fixed-dose artesunate-amodiaquine combination therapy in the treatment of uncomplicated Plasmodium falciparum malaria. *Malaria journal* **2009,** *8*, 125.
[19] Sagara, I., Rulisa, S., Mbacham, W., Adam, I., Sissoko, K., Maiga, H., Traore, O. B., Dara, N., Dicko, Y. T., Dicko, A., Djimde, A., Jansen, F. H., Doumbo, O. K., Efficacy and safety of a fixed dose artesunate-sulphamethoxypyrazine-pyrimethamine compared to artemether-lumefantrine for the treatment of uncomplicated falciparum malaria across Africa: a randomized multi-centre trial. *Malaria journal* **2009,** *8*, 63.
[20] Li, G. Q., Guo, X. B., Fu, L. C., Jian, H. X., Wang, X. H., Clinical trials of artemisinin and its derivatives in the treatment of malaria in China. *Transactions of the Royal Society of Tropical Medicine and Hygiene* **1994,** *88 Suppl 1*, S5-6.
[21] Tietche, F., Chelo, D., Mina Ntoto, N. K., Djoukoue, F. M., Hatz, C., Frey, S., Frentzel, A., Trapp, S., Zielonka, R., Mueller, E. A., Tolerability and efficacy of a pediatric granule formulation of artesunate-mefloquine in young children from Cameroon with uncomplicated falciparum malaria. *The American journal of tropical medicine and hygiene* **2010,** *82* (6), 1034-40.
[22] Tjitra, E., Hasugian, A. R., Siswantoro, H., Prasetyorini, B., Ekowatiningsih, R., Yusnita, E. A., Purnamasari, T., Driyah, S., Salwati, E., Nurhayati, Yuwarni, E., Januar, L., Labora, J., Wijayanto, B., Amansyah, F., Dedang, T. A., Purnama, A., Trihono, Efficacy and safety of artemisinin-naphthoquine versus dihydroartemisinin-piperaquine in adult patients with uncomplicated malaria: a multi-centre study in Indonesia. *Malaria journal* **2012,** *11*, 153.
[23] Gordi, T., Lepist, E. I., Artemisinin derivatives: toxic for laboratory animals, safe for humans? *Toxicology letters* **2004,** *147* (2), 99-107.
[24] Ribeiro, I. R., Olliaro, P., Safety of artemisinin and its derivatives. A review of published and unpublished clinical trials. *Medecine tropicale : revue du Corps de sante colonial* **1998,** *58* (3 Suppl), 50-3.
[25] Price, R., van Vugt, M., Phaipun, L., Luxemburger, C., Simpson, J., McGready, R., ter Kuile, F., Kham, A., Chongsuphajaisiddhi, T., White, N. J., Nosten, F., Adverse effects in patients with acute falciparum malaria treated with artemisinin derivatives. *The American journal of tropical medicine and hygiene* **1999,** *60* (4), 547-55.
[26] Brewer, T. G., Peggins, J. O., Grate, S. J., Petras, J. M., Levine, B. S., Weina, P. J., Swearengen, J., Heiffer, M. H., Schuster, B. G., Neurotoxicity in animals due to arteether and artemether. *Transactions of the Royal Society of Tropical Medicine and Hygiene* **1994,** *88 Suppl 1*, S33-6.

[27] Nontprasert, A., Nosten-Bertrand, M., Pukrittayakamee, S., Vanijanonta, S., Angus, B. J., White, N. J., Assessment of the neurotoxicity of parenteral artemisinin derivatives in mice. *The American journal of tropical medicine and hygiene* **1998,** *59* (4), 519-22.
[28] Morris, C. A., Duparc, S., Borghini-Fuhrer, I., Jung, D., Shin, C. S., Fleckenstein, L., Review of the clinical pharmacokinetics of artesunate and its active metabolite dihydroartemisinin following intravenous, intramuscular, oral or rectal administration. *Malaria journal* **2011,** *10*, 263.
[29] Batty, K. T., Thu, L. T., Davis, T. M., Ilett, K. F., Mai, T. X., Hung, N. C., Tien, N. P., Powell, S. M., Thien, H. V., Binh, T. Q., Kim, N. V., A pharmacokinetic and pharmacodynamic study of intravenous vs oral artesunate in uncomplicated falciparum malaria. *British journal of clinical pharmacology* **1998,** *45* (2), 123-9.
[30] Batty, K. T., Le, A. T., Ilett, K. F., Nguyen, P. T., Powell, S. M., Nguyen, C. H., Truong, X. M., Vuong, V. C., Huynh, V. T., Tran, Q. B., Nguyen, V. M., Davis, T. M., A pharmacokinetic and pharmacodynamic study of artesunate for vivax malaria. *The American journal of tropical medicine and hygiene* **1998,** *59* (5), 823-7.
[31] Teja-Isavadharm, P., Watt, G., Eamsila, C., Jongsakul, K., Li, Q., Keeratithakul, G., Sirisopana, N., Luesutthiviboon, L., Brewer, T. G., Kyle, D. E., Comparative pharmacokinetics and effect kinetics of orally administered artesunate in healthy volunteers and patients with uncomplicated falciparum malaria. *The American journal of tropical medicine and hygiene* **2001,** *65* (6), 717-21.
[32] Orrell, C., Little, F., Smith, P., Folb, P., Taylor, W., Olliaro, P., Barnes, K. I., Pharmacokinetics and tolerability of artesunate and amodiaquine alone and in combination in healthy volunteers. *European journal of clinical pharmacology* **2008,** *64* (7), 683-90.
[33] Davis, T. M., England, M., Dunlop, A. M., Page-Sharp, M., Cambon, N., Keller, T. G., Heidecker, J. L., Ilett, K. F., Assessment of the effect of mefloquine on artesunate pharmacokinetics in healthy male volunteers. *Antimicrobial agents and chemotherapy* **2007,** *51* (3), 1099-101.
[34] Tan, B., Naik, H., Jang, I. J., Yu, K. S., Kirsch, L. E., Shin, C. S., Craft, J. C., Fleckenstein, L., Population pharmacokinetics of artesunate and dihydroartemisinin following single- and multiple-dosing of oral artesunate in healthy subjects. *Malaria journal* **2009,** *8*, 304.
[35] Efferth, T., Dunstan, H., Sauerbrey, A., Miyachi, H., Chitambar, C. R., The anti-malarial artesunate is also active against cancer. *International journal of oncology* **2001,** *18* (4), 767-73.
[36] Woerdenbag, H. J., Moskal, T. A., Pras, N., Malingre, T. M., el-Feraly, F. S., Kampinga, H. H., Konings, A. W., Cytotoxicity of artemisinin-related endoperoxides to Ehrlich ascites tumor cells. *Journal of natural products* **1993,** *56* (6), 849-56.
[37] Jung, M., Lee, S., Ham, J., Lee, K., Kim, H., Kim, S. K., Antitumor activity of novel deoxoartemisinin monomers, dimers, and trimer. *Journal of medicinal chemistry* **2003,** *46* (6), 987-94.
[38] Dell'Eva, R., Pfeffer, U., Vene, R., Anfosso, L., Forlani, A., Albini, A., Efferth, T., Inhibition of angiogenesis in vivo and growth of Kaposi's sarcoma

xenograft tumors by the anti-malarial artesunate. *Biochemical pharmacology* **2004,** *68* (12), 2359-66.

[39] Hou, J., Wang, D., Zhang, R., Wang, H., Experimental therapy of hepatoma with artemisinin and its derivatives: in vitro and in vivo activity, chemosensitization, and mechanisms of action. *Clinical cancer research* **2008,** *14* (17), 5519-30.

[40] Lai, H., Nakase, I., Lacoste, E., Singh, N. P., Sasaki, T., Artemisinin-transferrin conjugate retards growth of breast tumors in the rat. *Anticancer research* **2009,** *29* (10), 3807-10.

[41] Zhang, Z. Y., Yu, S. Q., Miao, L. Y., Huang, X. Y., Zhang, X. P., Zhu, Y. P., Xia, X. H., Li, D. Q., Artesunate combined with vinorelbine plus cisplatin in treatment of advanced non-small cell lung cancer: a randomized controlled trial. *Journal of Chinese integrative medicine* **2008,** *6* (2), 134-8 (Abstract).

[42] Berger, T. G., Dieckmann, D., Efferth, T., Schultz, E. S., Funk, J. O., Baur, A., Schuler, G., Artesunate in the treatment of metastatic uveal melanoma--first experiences. *Oncology reports* **2005,** *14* (6), 1599-603.

[43] Singh, N. P., Verma, K. B., Case report of a laryngeal squamous cell carcinoma treated with artesunate. *Archive of oncology* **2002,** *10* (4), 279-80.

[44] Singh, N. P., Panwar, V. K., Case report of a pituitary macroadenoma treated with artemether. *Integrative cancer therapies* **2006,** *5* (4), 391-4.

[45] Crespo-Ortiz, M. P., Wei, M. Q., Antitumor activity of artemisinin and its derivatives: from a well-known antimalarial agent to a potential anticancer drug. *Journal of biomedicine & biotechnology* **2012,** *2012*, 247597.

[46] Efferth, T., Molecular pharmacology and pharmacogenomics of artemisinin and its derivatives in cancer cells. *Current drug targets* **2006,** *7* (4), 407-21.

[47] Kwok, J. C., Richardson, D. R., The iron metabolism of neoplastic cells: alterations that facilitate proliferation? *Critical reviews in oncology/hematology* **2002,** *42* (1), 65-78.

[48] Mercer, A. E., Copple, I. M., Maggs, J. L., O'Neill, P. M., Park, B. K., The role of heme and the mitochondrion in the chemical and molecular mechanisms of mammalian cell death induced by the artemisinin antimalarials. *The Journal of biological chemistry* **2011,** *286* (2), 987-96.

[49] Kelter, G., Steinbach, D., Konkimalla, V. B., Tahara, T., Taketani, S., Fiebig, H. H., Efferth, T., Role of transferrin receptor and the ABC transporters ABCB6 and ABCB7 for resistance and differentiation of tumor cells towards artesunate. *PloS one* **2007,** *2* (8), e798.

[50] Singh, N. P., Lai, H., Selective toxicity of dihydroartemisinin and holotransferrin toward human breast cancer cells. *Life sciences* **2001,** *70* (1), 49-56.

[51] Moore, J. C., Lai, H., Li, J. R., Ren, R. L., McDougall, J. A., Singh, N. P., Chou, C. K., Oral administration of dihydroartemisinin and ferrous sulfate retarded implanted fibrosarcoma growth in the rat. *Cancer letters* **1995,** *98* (1), 83-7.

[52] Hacker, M., Bachmann, K., Messer, W., Pharmacology - Principles and Practice; Chapter 8 Drug Metabolism. Elsevier, Burlington, MA: **2009**; pp. 130-173.

[53] Roederer, M. W., Cytochrome P450 enzymes and genotype-guided drug therapy. *Current opinion in molecular therapeutics* **2009,** *11* (6), 632-40.

[54] Pelkonen, O., Turpeinen, M., Hakkola, J., Honkakoski, P., Hukkanen, J., Raunio, H., Inhibition and induction of human cytochrome P450 enzymes: current status. *Archives of toxicology* **2008,** *82* (10), 667-715.
[55] Ward, B. A., Gorski, J. C., Jones, D. R., Hall, S. D., Flockhart, D. A., Desta, Z., The cytochrome P450 2B6 (CYP2B6) is the main catalyst of efavirenz primary and secondary metabolism: implication for HIV/AIDS therapy and utility of efavirenz as a substrate marker of CYP2B6 catalytic activity. *The Journal of pharmacology and experimental therapeutics* **2003,** *306* (1), 287-300.
[56] Hidestrand, M., Oscarson, M., Salonen, J. S., Nyman, L., Pelkonen, O., Turpeinen, M., Ingelman-Sundberg, M., CYP2B6 and CYP2C19 as the major enzymes responsible for the metabolism of selegiline, a drug used in the treatment of Parkinson's disease, as revealed from experiments with recombinant enzymes. *Drug metabolism and disposition: the biological fate of chemicals* **2001,** *29* (11), 1480-4.
[57] Turpeinen, M., Raunio, H., Pelkonen, O., The functional role of CYP2B6 in human drug metabolism: substrates and inhibitors in vitro, in vivo and in silico. *Current drug metabolism* **2006,** *7* (7), 705-14.
[58] Zanger, U. M., Klein, K., Pharmacogenetics of cytochrome P450 2B6 (CYP2B6): advances on polymorphisms, mechanisms, and clinical relevance. *Frontiers in genetics* **2013,** *4*, 24.
[59] Svensson, U. S., Ashton, M., Identification of the human cytochrome P450 enzymes involved in the in vitro metabolism of artemisinin. *British journal of clinical pharmacology* **1999,** *48* (4), 528-35.
[60] Honda, M., Muroi, Y., Tamaki, Y., Saigusa, D., Suzuki, N., Tomioka, Y., Matsubara, Y., Oda, A., Hirasawa, N., Hiratsuka, M., Functional characterization of CYP2B6 allelic variants in demethylation of antimalarial artemether. *Drug metabolism and disposition: the biological fate of chemicals* **2011,** *39* (10), 1860-5.
[61] Wienkers, L. C., Heath, T. G., Predicting in vivo drug interactions from in vitro drug discovery data. *Nature reviews. Drug discovery* **2005,** *4* (10), 825-33.
[62] Barry, M., Feely, J., Enzyme induction and inhibition. *Pharmacology & therapeutics* **1990,** *48* (1), 71-94.
[63] Hollenberg, P. F., Characteristics and common properties of inhibitors, inducers, and activators of CYP enzymes. *Drug metabolism reviews* **2002,** *34* (1-2), 17-35.
[64] Ashton, M., Hai, T. N., Sy, N. D., Huong, D. X., Van Huong, N., Nieu, N. T., Cong, L. D., Artemisinin pharmacokinetics is time-dependent during repeated oral administration in healthy male adults. *Drug metabolism and disposition* **1998,** *26* (1), 25-7.
[65] Ashton, M., Nguyen, D. S., Nguyen, V. H., Gordi, T., Trinh, N. H., Dinh, X. H., Nguyen, T. N., Le, D. C., Artemisinin kinetics and dynamics during oral and rectal treatment of uncomplicated malaria. *Clinical pharmacology and therapeutics* **1998,** *63* (4), 482-93.
[66] Gordi, T., Huong, D. X., Hai, T. N., Nieu, N. T., Ashton, M., Artemisinin pharmacokinetics and efficacy in uncomplicated-malaria patients treated with two different dosage regimens. *Antimicrobial agents and chemotherapy* **2002,** *46* (4), 1026-31.

[67] Simonsson, U. S., Jansson, B., Hai, T. N., Huong, D. X., Tybring, G., Ashton, M., Artemisinin autoinduction is caused by involvement of cytochrome P450 2B6 but not 2C9. *Clinical pharmacology and therapeutics* **2003,** *74* (1), 32-43.
[68] Burk, O., Arnold, K. A., Nussler, A. K., Schaeffeler, E., Efimova, E., Avery, B. A., Avery, M. A., Fromm, M. F., Eichelbaum, M., Antimalarial artemisinin drugs induce cytochrome P450 and MDR1 expression by activation of xenosensors pregnane X receptor and constitutive androstane receptor. *Molecular pharmacology* **2005,** *67* (6), 1954-65.
[69] Brandon, E. F., Raap, C. D., Meijerman, I., Beijnen, J. H., Schellens, J. H., An update on in vitro test methods in human hepatic drug biotransformation research: pros and cons. *Toxicology and applied pharmacology* **2003,** *189* (3), 233-46.
[70] Baranczewski, P., Stanczak, A., Sundberg, K., Svensson, R., Wallin, A., Jansson, J., Garberg, P., Postlind, H., Introduction to in vitro estimation of metabolic stability and drug interactions of new chemical entities in drug discovery and development. *Pharmacological Reports* **2006,** *58* (4), 453-72.
[71] Ito, K., Brown, H. S., Houston, J. B., Database analyses for the prediction of in vivo drug-drug interactions from in vitro data. *British journal of clinical pharmacology* **2004,** *57* (4), 473-86.
[72] Bachmann, K. A., Inhibition constants, inhibitor concentrations and the prediction of inhibitory drug drug interactions: pitfalls, progress and promise. *Current drug metabolism* **2006,** *7* (1), 1-14.
[73] Graham, G. G., Noninvasive chemical methods of estimating pharmacokinetic parameters. *Pharmacology & therapeutics* **1982,** *18* (3), 333-49.
[74] Ruiz, M. E., Conforti, P., Fagiolino, P., Volonte, M. G., The use of saliva as a biological fluid in relative bioavailability studies: comparison and correlation with plasma results. *Biopharmaceutics & drug disposition* **2010,** *31* (8-9), 476-85.
[75] Jusko, W. J., Milsap, R. L., Pharmacokinetic principles of drug distribution in saliva. *Annals of the New York Academy of Sciences* **1993,** *694*, 36-47.
[76] Trnavska, Z., Krejcova, H., Tkaczykovam, Salcmanova, Z., Elis, J., Pharmacokinetics of lamotrigine (Lamictal) in plasma and saliva. *European journal of drug metabolism and pharmacokinetics* **1991,** *Spec No 3*, Abstract.
[77] Graham, G., Rowland, M., Application of salivary salicylate data to biopharmaceutical studies of salicylates. *Journal of pharmaceutical sciences* **1972,** *61* (8), 1219-22.
[78] Koysooko, R., Ellis, E. F., Levy, G., Relationship between theophylline concentration in plasma and saliva of man. *Clinical pharmacology and therapeutics* **1974,** *15* (5), 454-60.
[79] Inaba, T., Kalow, W., Salivary excretion of amobarbital in man. *Clinical pharmacology and therapeutics* **1975,** *18* (5 Pt 1), 558-62.
[80] Sidhu, J. S., Ashton, M., Single-dose, comparative study of venous, capillary and salivary artemisinin concentrations in healthy, male adults. *The American journal of tropical medicine and hygiene* **1997,** *56* (1), 13-6.
[81] Gordi, T., Hai, T. N., Hoai, N. M., Thyberg, M., Ashton, M., Use of saliva and capillary blood samples as substitutes for venous blood sampling in

pharmacokinetic investigations of artemisinin. *European journal of clinical pharmacology* **2000,** *56* (8), 561-6.
[82] Bansal, S., DeStefano, A., Key elements of bioanalytical method validation for small molecules. *The AAPS journal* **2007,** *9* (1), E109-14.
[83] *Guidance for Industry: Bioanalytical Method Validation*. U.S. Food and Drug Administration, **2001**
[84] Williams, P., Ette, E., Pharmacometrics: impacting drug development and pharmacotherapy. In *Pharmacometrics: The Science of Quantitative Pharmacology.* Williams, P.; Ette, E., Eds. John Wiley & Sons, Hoboken, NJ: 2007; pp 1-21.
[85] *Guidance for Industry: Population Pharmacokinetics*. U.S. Food and Drug Administration, **1999**
[86] Grasela, T. H., Sheiner, L. B., Pharmacostatistical modeling for observational data. *Journal of Pharmacokinetics and Biopharmaceutics* **1991,** *19* (3), 25-36.
[87] Beal, S. L., Sheiner, L. B., *NONMEM users guides*. NONMEM Project Group, University of San Francisco, CA. **1998**
[88] Kim, M. J., Kim, H., Cha, I. J., Park, J. S., Shon, J. H., Liu, K. H., Shin, J. G., High-throughput screening of inhibitory potential of nine cytochrome P450 enzymes in vitro using liquid chromatography/tandem mass spectrometry. *Rapid communications in mass spectrometry : RCM* **2005,** *19* (18), 2651-8.
[89] Ito, K., Iwatsubo, T., Kanamitsu, S., Ueda, K., Suzuki, H., Sugiyama, Y., Prediction of pharmacokinetic alterations caused by drug-drug interactions: metabolic interaction in the liver. *Pharmacological reviews* **1998,** *50* (3), 387-412.
[90] Lindbom, L., Pihlgren, P., Jonsson, E. N., PsN-Toolkit--a collection of computer intensive statistical methods for non-linear mixed effect modeling using NONMEM. *Computer methods and programs in biomedicine* **2005,** *79* (3), 241-57.
[91] Lindbom, L., Ribbing, J., Jonsson, E. N., Perl-speaks-NONMEM (PsN)--a Perl module for NONMEM related programming. *Computer methods and programs in biomedicine* **2004,** *75* (2), 85-94.
[92] Jonsson, E. N., Karlsson, M. O., Xpose--an S-PLUS based population pharmacokinetic/pharmacodynamic model building aid for NONMEM. *Computer methods and programs in biomedicine* **1999,** *58* (1), 51-64.
[93] Efferth, T., Kaina, B., Toxicity of the antimalarial artemisinin and its dervatives. *Critical reviews in toxicology* **2010,** *40* (5), 405-21.
[94] National Cancer Institute at the National Institutes of Health Breast Cancer Treatment.
http://www.cancer.gov/cancertopics/pdq/treatment/breast/Patient/page5#Keypoint24 (accessed May 30, **2014**).
[95] Crewe, H. K., Notley, L. M., Wunsch, R. M., Lennard, M. S., Gillam, E. M., Metabolism of tamoxifen by recombinant human cytochrome P450 enzymes: formation of the 4-hydroxy, 4'-hydroxy and N-desmethyl metabolites and isomerization of trans-4-hydroxytamoxifen. *Drug metabolism and disposition: the biological fate of chemicals* **2002,** *30* (8), 869-74.
[96] Ilett, K. F., Ethell, B. T., Maggs, J. L., Davis, T. M., Batty, K. T., Burchell, B., Binh, T. Q., Thu le, T. A., Hung, N. C., Pirmohamed, M., Park, B. K., Edwards, G., Glucuronidation of dihydroartemisinin in vivo and by human liver microsomes

and expressed UDP-glucuronosyltransferases. *Drug metabolism and disposition: the biological fate of chemicals* **2002,** *30* (9), 1005-12.

[97] Gallicano, K. D., Sahai, J., Shukla, V. K., Seguin, I., Pakuts, A., Kwok, D., Foster, B. C., Cameron, D. W., Induction of zidovudine glucuronidation and amination pathways by rifampicin in HIV-infected patients. *British journal of clinical pharmacology* **1999,** *48* (2), 168-79.

[98] Ouellet, D., Hsu, A., Qian, J., Locke, C. S., Eason, C. J., Cavanaugh, J. H., Leonard, J. M., Granneman, G. R., Effect of ritonavir on the pharmacokinetics of ethinyl oestradiol in healthy female volunteers. *British journal of clinical pharmacology* **1998,** *46* (2), 111-6.

[99] Leskovac, V., Theoharides, A. D., Hepatic metabolism of artemisinin drugs--I. Drug metabolism in rat liver microsomes. *Comparative biochemistry and physiology. C, Comparative pharmacology and toxicology* **1991,** *99* (3), 383-90.

[100] Liu, T., Du, F., Wan, Y., Zhu, F., Xing, J., Rapid identification of phase I and II metabolites of artemisinin antimalarials using LTQ-Orbitrap hybrid mass spectrometer in combination with online hydrogen/deuterium exchange technique. *Journal of mass spectrometry : JMS* **2011,** *46* (8), 725-33.

[101] The Human Metabolome Database (HMDB). http://www.hmdb.ca/metabolites/HMDB61088 (accessed 2 June, **2014**).

[102] Augustijns, P., D'Hulst, A., Van Daele, J., Kinget, R., Transport of artemisinin and sodium artesunate in Caco-2 intestinal epithelial cells. *Journal of pharmaceutical sciences* **1996,** *85* (6), 577-9.

[103] Batty, K. T., Ilett, K. F., Davis, T. M., Protein binding and alpha : beta anomer ratio of dihydroartemisinin in vivo. *British journal of clinical pharmacology* **2004,** *57* (4), 529-33.

[104] Dondorp, A. M., Nosten, F., Yi, P., Das, D., Phyo, A. P., Tarning, J., Lwin, K. M., Ariey, F., Hanpithakpong, W., Lee, S. J., Ringwald, P., Silamut, K., Imwong, M., Chotivanich, K., Lim, P., Herdman, T., An, S. S., Yeung, S., Singhasivanon, P., Day, N. P., Lindegardh, N., Socheat, D., White, N. J., Artemisinin resistance in Plasmodium falciparum malaria. *The New England journal of medicine* **2009,** *361* (5), 455-67.

[105] Phyo, A. P., Nkhoma, S., Stepniewska, K., Ashley, E. A., Nair, S., McGready, R., ler Moo, C., Al-Saai, S., Dondorp, A. M., Lwin, K. M., Singhasivanon, P., Day, N. P., White, N. J., Anderson, T. J., Nosten, F., Emergence of artemisinin-resistant malaria on the western border of Thailand: a longitudinal study. *Lancet* **2012,** *379* (9830), 1960-6.

SUPPLEMENTARY MATERIALS

Paper III – Bioanalytical method for quantification of ARS and DHA in human plasma and saliva

Supplement 1. Back-calculated concentrations of standard curves for artesunate (ARS) and dihydroartemisinin (DHA) in human plasma. Average concentrations (n=8) and standard deviations (SD) presented in ng/mL and precision by the %CV.

	Nominal concentration					
	5 ng/mL	15 ng/mL	50 ng/mL	100 ng/mL	500 ng/mL	1000 ng/mL
ARS						
Average	5.02	14.8	50.2	99.5	507	993
SD	0.07	0.80	3.27	4.37	14.7	13.9
CV (%)	1.41	5.43	6.51	4.39	2.91	1.40
Accuracy	100	98.8	101	99.5	102	99.3
	Nominal concentration					
	5 ng/mL	15 ng/mL	50 ng/mL	250 ng/mL	1000 ng/mL	2000 ng/mL
DHA						
Average	5.04	14.8	49.4	253	1020	1980
SD	0.06	0.55	2.49	8.48	46.0	42.8
CV (%)	1.24	3.73	5.03	3.36	4.51	2.16
Accuracy	101	98.9	98.8	101	102.	99.0

Supplement 2. Back-calculated concentrations of standard curves for artesunate (ARS) and dihydroartemisinin (DHA) in human saliva. Average concentrations (n=8) and standard deviations (SD) presented in ng/mL and precision by the %CV.

	Nominal concentration					
	5 ng/mL	15 ng/mL	50 ng/mL	100 ng/mL	500 ng/mL	1000 ng/mL
ARS						
Average	4.69	15.0	50.1	99.6	501	1001
SD	0.88	0.36	1.23	2.90	14.3	15.0
CV (%)	18.8	2.39	2.46	2.91	2.86	1.50
Accuracy	93.8	100	100	99.6	100	100
	Nominal concentration					
	5 ng/mL	15 ng/mL	50 ng/mL	250 ng/mL	1000 ng/mL	2000 ng/mL
DHA						
Average	4.68	15.0	50.5	245	1016	1986
SD	0.88	0.21	0.92	5.64	13.6	9.16
CV (%)	18.8	1.38	1.82	2.30	1.34	0.46
Accuracy	93.7	100	101	98.1	102	99.3

Paper V – Population pharmacokinetics of ARS and DHA in patients with breast cancer

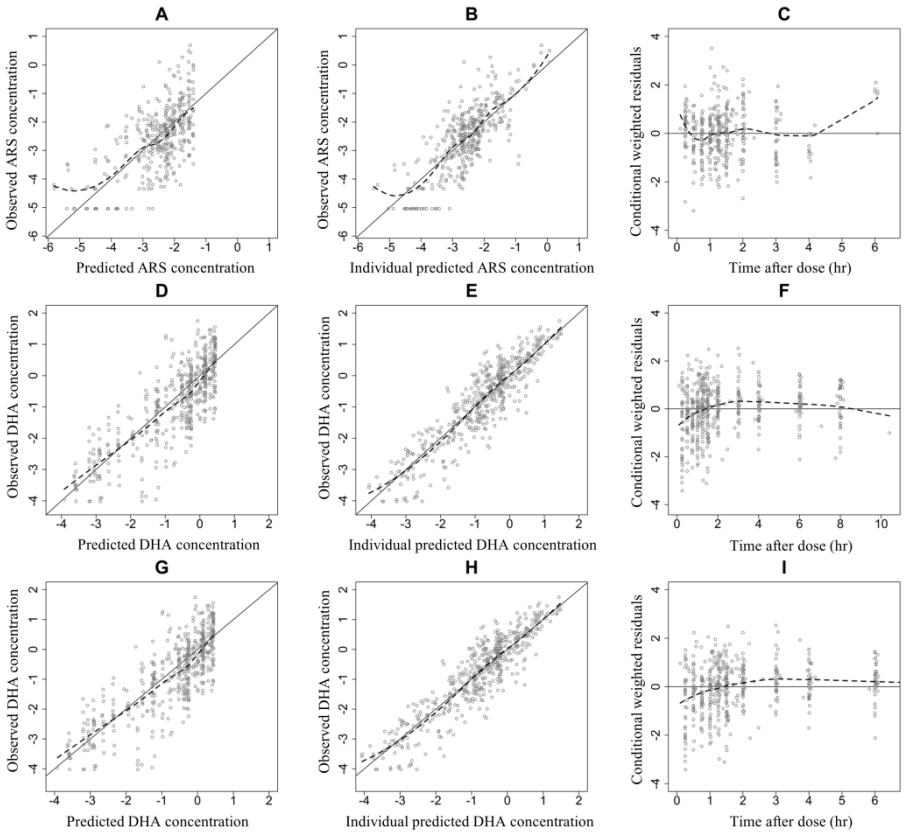

Supplement 1. Basic goodness-of-fit plots for artesunate (ARS) in plasma (A, B, C), dihydroartemisinin (DHA) in plasma (D, E, F), and DHA in saliva (G, H, I) using model A and full concentration-time profile data plus sparse sample data. Observed concentrations plotted against population predicted concentrations (A, D, G) and individual predicted concentrations (B, E, H), respectively. Conditional weighted residuals plotted against time after dose (C, F, H). Time axes are truncated to 6.5 hours for plasma ARS and salivary DHA, and to 10.5 hours for plasma DHA, respectively. Solid lines represent the identity lines and the dashed lines are the locally weighted least square regression lines. All concentrations are represented as transformed values using the natural logarithm. Observed ARS plasma concentrations equal to -5.04 seen in the lower part of plot A and B, represent the BQL data that was imputed as LLOQ/2.

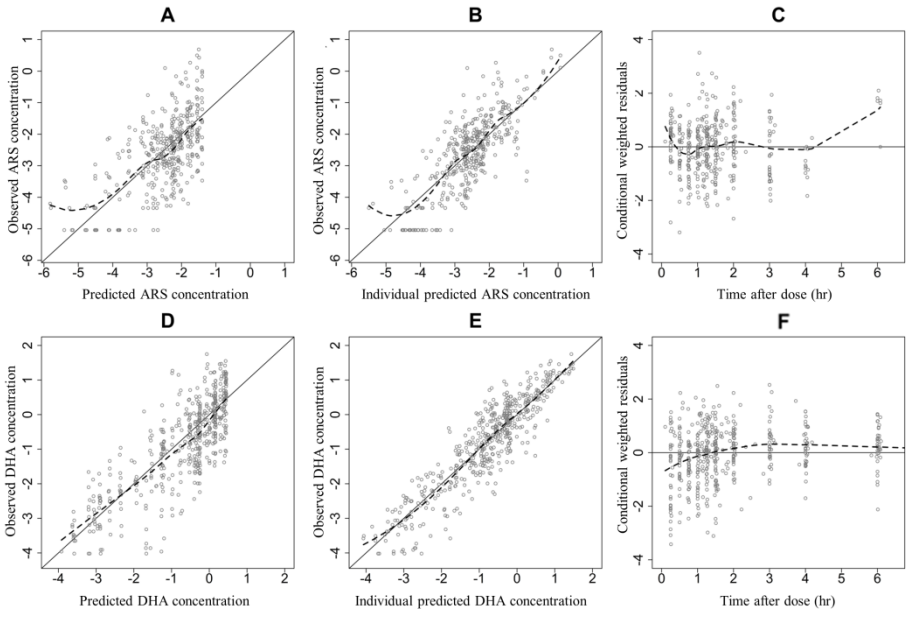

Supplement 2. Basic goodness-of-fit plots for plasma artesunate (ARS) (A, B, C) and dihydroartemisinin (DHA) (D, E, F) using model B and only full concentration-time profile data. Observed concentrations plotted against population predicted concentrations (A, D) and individual predicted concentrations (B, E), respectively. Conditional weighted residuals plotted against time after dose (C, F). Time axes are truncated to 6.5 and 8.5 hours for ARS and DHA, respectively. Solid lines represent the identity lines and the dashed lines are the locally weighted least square regression lines. All concentrations are represented as transformed values using the natural logarithm. Observed ARS plasma concentrations equal to -5.04 seen in the lower part of plot A and B, represent the BQL data that was imputed as LLOQ/2.